trends. There was no evidence of secondary extinction in the low-angle, high-intensity data, save for one reflection (021) that seemed badly affected. Since other reflections of nearly the same intensity were not, no correction was performed. The largest peak in the final difference Fourier map had an electron density of 0.23 $e^-/Å^3$. The positional and thermal parameters for **20** and a listing of the values of F_o and F_c are available as supplementary material.

Acknowledgment. We are grateful to Professor H. Werner for communicating research results to us prior to publication and to a referee for a very thorough reading of the manuscript and a number of helpful suggestions (especially on nomenclature). Financial support for this work was provided by National Science Foundation Grant CHE79-26291. W.H.H. acknowledges an NIH National Research Service Award (F32-GM-07539) from the National Institute of General Medical Sciences. The crystal structure analyses were performed at the U. C. Berkeley X-ray Crystallographic Facility (CHEXRAY). Funds for the analyses were provided by the above NIH grant; partial funding for the equipment in the facility was provided by the NSF through Grant CHE79-07027. R.G.B. acknowledges a Research Professorship (1982-1983) from the Miller Institute for Basic Research at U. C. Berkeley.

Registry No. 1, 79931-94-5; **2**, 62602-00-0; **3**, 58496-39-2; **7**, 86364-94-5; **8**, 86364-95-6; **10**, 12078-25-0; **11**, 79931-95-6; **12**, 1271-08-5; **13**, 615-13-4; **14**, 4968-91-6; **15**, 1460-59-9; **16**, 12203-85-9; **19**, 86364-96-7; **20**, 86364-97-8; $MeCpCo(CO)_2$, 75297-02-8; $MeCpCo(CO)PPhMe_2$, 86364-98-9; $[CpCo(CO)]_2$(diphos), 86365-00-6; CpCo(diphos), 86365-01-7; α,α'-dibromo-*o*-xylylene, 91-13-4; (μ-*o*-xylylene)bis(η^5-cyclopentadienyl)dicobalt, 86364-99-0.

Supplementary Material Available: For compounds **8**, **11**, and **20**, positional and thermal parameters and their estimated standard deviations, general temperature factor expressions, *B*'s, and listings of observed and calculated structure factors (38 pages). Ordering information is given on any current masthead page.

Kinetics and Mechanism of Decomposition of a Benzodicobaltacyclohexene: Reversible Dinuclear Elimination of *o*-Xylylene via a Dimetalla-Diels-Alder Reaction

William H. Hersh and Robert G. Bergman*

Contribution from the Department of Chemistry, University of California, Berkeley, California 94720. *Received December 27, 1982*

Abstract: A detailed mechanistic study of several reactions of the first dimetallacyclohexene, $(\eta^5\text{-Cp})_2Co_2(\mu\text{-CO})_2(\mu\text{-}o\text{-xylylene})$ (**1**), is described. The predominant reaction pathway is proposed to involve reversible cleavage of **1** in Diels-Alder fashion, into free *o*-xylylene (**3**) and the metal-metal double-bonded dimer **9**. Several lines of evidence support this conclusion. Crossover experiments demonstrated that loss of **3** from **1** in its reaction with $PPhMe_2$ to give dinuclear monophosphine adduct **2** is a dinuclear elimination process that leaves the cobalt-cobalt bond intact. Kinetic studies showed that sufficiently high concentrations of several ligands (phosphines, bis(methylcyclopentadienyl) metal-metal double-bonded dimer **10**, or dimethyl acetylenedicarboxylate (DMAD)) induce decomposition of **1** at the same maximum rate, to give monophosphine adduct **2**, bis(methylcyclopentadienyl) dimetallacyclohexene **5**, or dinuclear DMAD adduct **16**, respectively. Both the phosphine and DMAD reactions exhibited falloff in the observed rates of decomposition at lower ligand concentration. On the basis of the proposal that **1** was in thermal equilibrium with two reactive intermediates (**3** and **9**), theoretical results suggested, and were experimentally confirmed, that at low DMAD concentration the falloff in decomposition rate could be eliminated by lowering the concentration of **1**, to again induce decomposition at the previously observed maximum rate. An Arrhenius plot of data collected in this limiting rate regime, representing the rate of the retro-dimetalla-Diels-Alder reaction, gave $\Delta H^{\ddagger} = 24.3$ kcal/mol and $\Delta S^{\ddagger} = +12.1$ eu. Preparative reactions of double-bonded dimer **9** with two different *o*-xylylene precursors gave moderate yields of metallacycle **1**, providing additional evidence for the forward dimetalla-Diels-Alder reaction. A minor reaction pathway, thermal decomposition of **1** to CpCo(*o*-xylylene) (**12**) and $CpCo(CO)_2$ (**13**), was also observed. Evidence is presented suggesting that it is mechanistically related to the major decomposition pathway operating in other dinuclear dicobalt systems, involving intramolecular alkyl to cobalt migration.

The recent surge in interest in the chemistry of transition-metal cluster compounds has been fueled by the notion that the behavior of these materials may model that found at metal surfaces.[1] One reason for wanting to model surface reactions is that certain heterogeneous reactions, such as the Fischer-Tropsch reaction and C-H and C-C bond activation, have so far been duplicated only rarely in solution.[2-4] Since a reason for this difficulty may be that more than one metal center in some cases is needed to effect such reactions, metal clusters are obvious candidates for

Scheme I

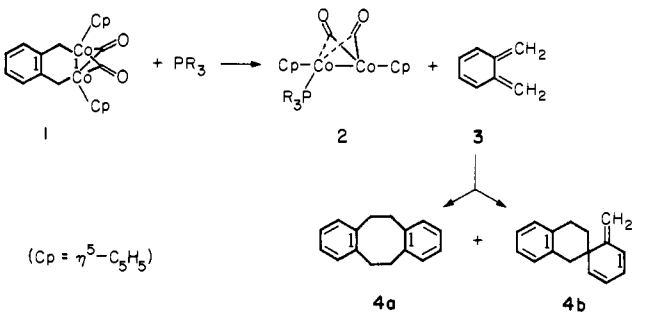

(1) (a) Muetterties, E. L. *Bull. Soc. Chim. Belg.* **1975**, *84*, 959-986. (b) Lewis, J.; Johnson, B. F. G. *Pure Appl. Chem.* **1975**, *44*, 43-79. (c) Muetterties E. L.; Stein, J. *Chem. Rev.* **1979**, *79*, 479-490.

(2) For homogeneous Fischer-Tropsch reactions, see: (a) Thomas, M. G.; Beier, B. F.; Muetterties, E. L. *J. Am. Chem. Soc.* **1976**, *98*, 1296-1297. (b) Demitras, G. C.; Muetterties, E. L. *Ibid.* **1977**, *99*, 2796-2797. (c) Perkins, P.; Vollhardt, K. P. C. *Ibid.* **1979**, *101*, 3985-3987. (d) For a demonstration that a system thought to display Fischer-Tropsch chemistry in fact does not, see: Benner, L. S.; Lai, Y. H.; Vollhardt, K. P. C. *Ibid.* **1981**, *103*, 3609-3611.

0002-7863/83/1505-5846$01.50/0

Scheme II

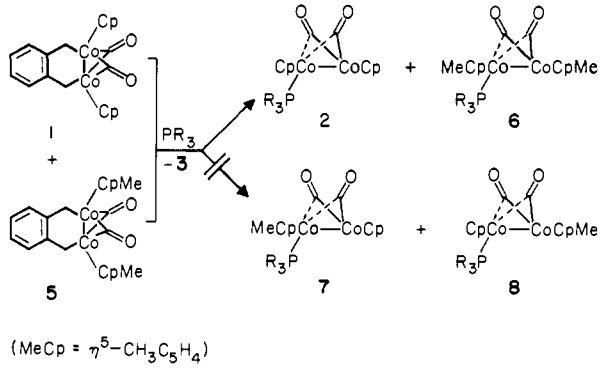

(MeCp = η^5-$CH_3C_5H_4$)

inducing them homogeneously. An assumption inherent in this hypothesis concerns the nuclearity of the reactions induced by the clusters. The cluster can only serve as a surface model if it remains intact throughout the course of the reaction. In other words, new chemistry that is without analogy in mononuclear systems may be anticipated only if cluster fragmentation does not occur, since the chemistry so induced might be due only to mononuclear (albeit reactive) species.

Dinuclear metal–metal bonded species represent the simplest systems in which one may consider the question of cluster fragmentation. We have been interested in a series of dialkyldicobalt compounds, in which both CO insertion and reductive elimination reactions have been observed.[5] However, rearrangement to mononuclear or non-metal–metal bonded intermediates occurs competitively with the carbon–carbon bond-forming steps in many of these reactions.[5e,6] Hence, it has not been possible to determine whether any of the mechanisms are dinuclear.[7]

In the accompanying paper we described the synthesis, structural characterizations, and reactions of benzodicobaltacyclohexene **1**.[8] One of its reactions was of particular mechanistic interest, namely, that with phosphines to give dinuclear monophosphine adduct **2** and free *o*-xylylene (**3**), which rapidly dimerizes at room temperature to give **4** (Scheme I). This elimination of the organic part of the dimetallacycle, with apparent retention of the metal–metal bond in the initially formed organometallic product, represented our first opportunity to directly test whether or not a rare[9] *dinuclear* elimination was operative. We now report our findings that bear on this question as well as on the detailed mechanisms both of this elimination and several related reactions. Kinetic studies have allowed us to establish that all of these reactions proceed through an unusual type of bimolecular intermediate resulting from a dimetalla-retro-Diels–Alder reaction.

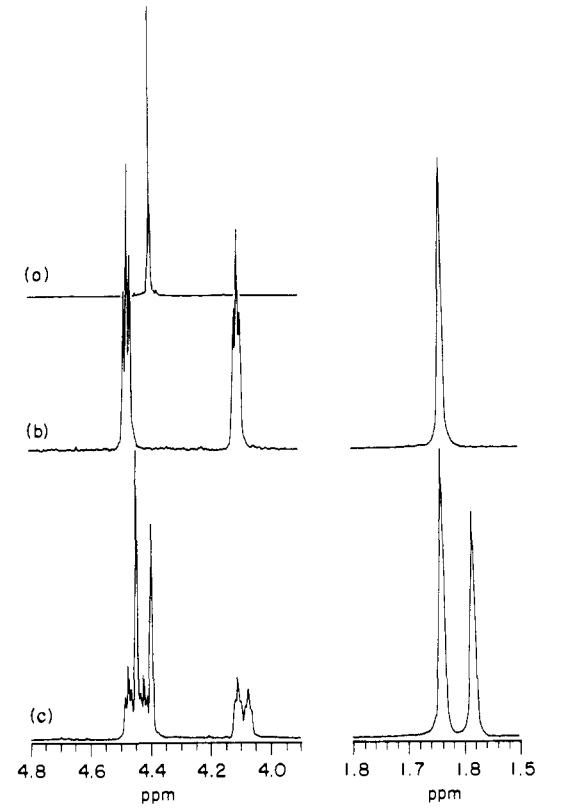

Figure 1. Cyclopentadienyl and methyl region of the ^{1}H NMR spectra of (a) $[CpCo(CO)]_2$ (**9**); (b) $[MeCpCo(CO)]_2$ (**10**); (c) a mixture of **9** and **10**; new peaks in the spectrum are due to mixed dimer (Cp)(MeCp)$Co_2(CO)_2$ (**11**).

Scheme III

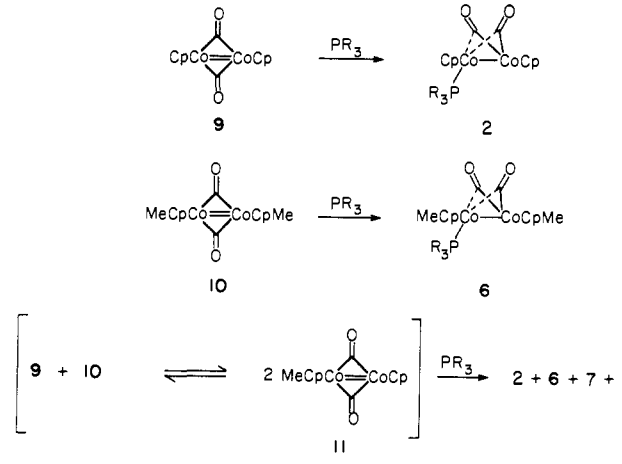

Table I. ^{1}H NMR Spectra[a] of Neutral Dimers 9-11

compd	Cp[b]	Me*Cp*[c]	Me*Cp*[d]	*Me*Cp[b]
9	4.40			
10		4.47	4.11	1.64
11	4.45	4.42	4.07	1.58

[a] C_6D_6 solution. [b] Signals are singlets. [c] Signals are triplets, J = 2.0 Hz. [d] Signals are triplets, J = 1.9 Hz.

Further evidence for this novel mechanism has been provided by observation of the forward dimetalla-Diels–Alder reaction, the first such observation of the organometallic analogue of this classic ring-forming reaction.

Results and Discussion

Phosphine-Addition and Cobalt-Interchange Reactions of $[CpCoCO]_2$ and $[MeCpCoCO]_2$ Dimers. An experiment which may

(3) For examples of homogeneous intermolecular C–H activation, see the following and references therein: (a) Crabtree, R. H.; Mihelcic, J. M.; Quirk, J. M. *J. Am. Chem. Soc.* **1979**, *101*, 7738–7740. (b) Baudry, D.; Ephritikine, M.; Felkin, H. *J. Chem. Soc., Chem. Commun.* **1980**, 1243–1244. (c) Crabtree, R. H.; Mellea, M. F.; Mihelcic, J. M.; Quirk, J. M. *J. Am. Chem. Soc.* **1982**, *104*, 107–113. (d) Janowicz, A. H.; Bergman, R. G. *Ibid.* **1982**, *104*, 352–354. (e) Graham, W. A. G.; Hoyano, J. K. *Ibid.* **1982**, *104*, 3723–3724. (f) Thorn, D. L. *Organometallics* **1982**, *1*, 197–204.

(4) For some examples of C–C activation, see: (a) Liebeskind, L. S.; Baysdon, S. L.; South, M. S.; Blount, J. F. *J. Organomet. Chem.* **1980**, *202*, C73–C76. (b) Eilbracht, P.; Dahler, P.; Mayser, U.; Henkes, E. *Chem. Ber.* **1980**, *113*, 1033–1046. (c) Puddephatt, R. J. *Coord. Chem. Rev.* **1980**, *33*, 149–194. (d) Suggs, J. W.; Cox, S. D. *J. Organomet. Chem.* **1981**, *221*, 199–201.

(5) (a) Schore, N. E.; Ilenda, C. S.; Bergman, R. G. *J. Am. Chem. Soc.* **1976**, *98*, 7436–7438. (b) Bryndza, H. E.; Bergman, R. G. *Ibid.* **1979**, *101*, 4766–4768. (c) White, M. A.; Bergman, R. G. *J. Chem. Soc., Chem. Commun.* **1979**, 1056–1058. (d) Theopold, K. H.; Bergman, R. G. *J. Am. Chem. Soc.* **1980**, *102*, 5694–5695. (e) Theopold, K. H.; Bergman, R. G. *Organometallics*, **1982**, *1*, 1571–1579.

(6) Bergman, R. G. *Acc. Chem. Res.* **1980**, *13*, 113–120.

(7) In some cases it has been possible to show that the observed CO insertion is in fact *not* dinuclear; see ref 6.

(8) Hersh, W. H.; Bergman, R. G., preceding paper in this issue.

(9) (a) Chetcuti, M. J.; Chisholm, M. H.; Folting, K.; Haitko, D. A.; Huffman, J. C. *J. Am. Chem. Soc.* **1982**, *104*, 2138–2146. (b) Halpern, J. *Inorg. Chim. Acta* **1982**, *62*, 31–37.

Scheme IV

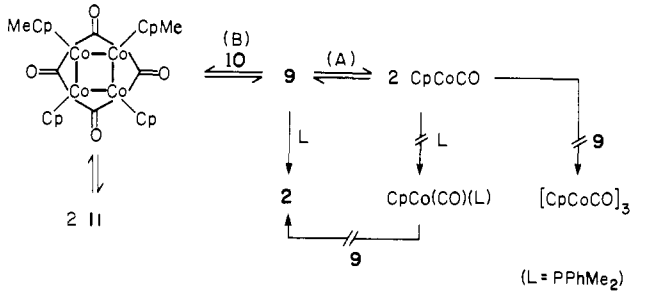

be used to examine the nuclearity of the reaction of **1** with phosphines is shown in Scheme II. If the reaction is truly dinuclear and if the cyclopentadienyl moieties remain attached to each cobalt, then reaction of a phosphine with a mixture of bis(cyclopentadienyl) complex **1** and bis(methylcyclopentadienyl) complex **5** will give rise only to the bis(cyclopentadienyl) and bis(methylcyclopentadienyl) phosphine adducts **2** and **6**. Observation of the crossover products **7** and **8** in addition to the unmixed products **2** and **6** would on the other hand indicate that some alternative intermolecular process was occurring.

In order to analyze the experiment shown in Scheme II it was first necessary to independently prepare mixed adducts **7** and **8**. The monophosphine adducts **2** and **6** are most conveniently and cleanly prepared by reaction of phosphines with the metal–metal double-bonded cobalt neutral dimers[8] **9** and **10** (Scheme III). It occurred to us that simple reaction of these two neutral dimers might give the desired mixed product (**11**) via a crossover reaction of the type that has been observed previously in (μ-alkylidene)dicobalt systems.[10] *In fact the reaction of* ***9*** *and* ***10*** *to* give ***11*** *occurs with amazing rapidity*, complete equilibration between **9**, **10**, and **11** being achieved in seconds at room temperature in C_6D_6 solution! The overall reaction can be observed conveniently by ^1H NMR, in which mixing **9** and **10** gives rise to a spectrum (Figure 1) containing signals due to **9** and **10** and four new signals due to **11** (Table I). Integration of an equilibrated mixture gave $K_{eq} = ([\mathbf{11}]^2/[\mathbf{9}][\mathbf{10}]) = 4.4$, indicating little if any thermodynamic preference for any particular dimer. An indication of the speed of the equilibration can be obtained by examination of the phosphine reaction with such mixtures. Thus, addition of $PPhMe_2$ to the above equilibrated mixture and integration of the resultant mixture of **2** and **6**–**8** (see below) gave $([\mathbf{7}]+[\mathbf{8}])^2/[\mathbf{2}][\mathbf{6}] = 4.9$, in good agreement with the directly measured value. However, mixing neutral dimers **9** and **10** on the order of 30–60 s followed by addition of $PPhMe_2$ gave $([\mathbf{7}]+[\mathbf{8}])^2/[\mathbf{2}][\mathbf{6}] = 2.1$, indicating that equilibration was already roughly 80–90% complete within that amount of time.

Two types of mechanisms that might account for the scrambling reaction of symmetrical Cp/Cp and MeCp/MeCp dimers **9** and **10** are shown in Scheme IV. Path A involves simple cleavage into CpCo(CO) and MeCpCo(CO) fragments followed by cross-recombination to give mixed Cp/MeCp dimer **11**. Such a mechanism would require an unusually high rate of recombination of these fragments, since (1) trapping by, for instance, neutral dimer **9** to give the more thermodynamically stable $[CpCo(CO)]_3$ is not observed and (2) trapping by phosphines to give $CpCo(CO)PR_3$ is not initially observed. Independent reaction of $MeCpCo(CO)PPhMe_2$ with dimer **9** does not result in formation of dinuclear phosphine adducts **7** or **8** (no reaction is observed within 2 h at room temperature) so this would not account for the failure to observe $CpCo(CO)PR_3$. The second type of mechanism (path B) involves a pairwise exchange reminiscent of the mechanisms initially proposed for the olefin metathesis reaction,[11] in which a tetrameric cobalt cluster can be envisioned

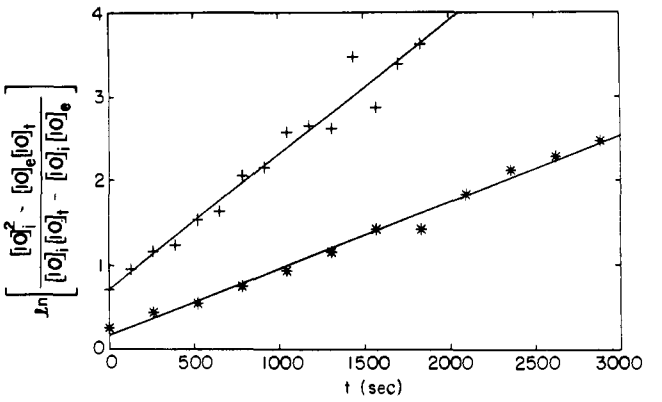

Figure 2. Plot of approach of [**10**] to its equilibrium concentration vs. time for two (excess) concentrations of **9** = 0.04 (*) and 0.012 M (+); the form of the log plot is given by eq 2.

as either a transition state or intermediate. In principle, these two possibilities should be readily distinguished, since the first would be unimolecular, the second bimolecular. In its simplest form, the reaction may be written as shown in eq 1; if one of the

$$\mathbf{9} + \mathbf{10} \underset{k_2}{\overset{k_1}{\rightleftharpoons}} \mathbf{211} \qquad (1)$$

reactants (**9**, here) is allowed to be present in "pseudo-first-order" excess, then the relatively simple integrated rate law shown in eq 2 is easily derived.[12] The values $[\mathbf{10}]_i$, $[\mathbf{10}]_t$, and $[\mathbf{10}]_e$ are the

$$\ln\left[\frac{1-\left(\frac{[\mathbf{10}]_e}{[\mathbf{10}]_i}\right)\left(\frac{[\mathbf{10}]_t}{[\mathbf{10}]_i}\right)}{\frac{[\mathbf{10}]_t}{[\mathbf{10}]_i}-\frac{[\mathbf{10}]_e}{[\mathbf{10}]_i}}\right] = k_1\left[\frac{1+\frac{[\mathbf{10}]_e}{[\mathbf{10}]_i}}{1-\frac{[\mathbf{10}]_e}{[\mathbf{10}]_i}}\right]t \qquad (2)$$

concentrations of **10** initially, at time t, and at equilibrium, while k_1 may be a function of [**9**]. It can be seen that as $[\mathbf{10}]_e$ approaches zero, the rate law (eq 2) takes on a simple first-order form, and therefore it is appropriate to describe the reaction in those terms.

A brief kinetic study of the scrambling reaction was therefore carried out to determine if the decomposition of MeCp neutral dimer **10** is indeed "first order" as described by eq 2 and if so whether or not the reaction is also first order in unsubstituted dimer **9**. In practice, experimental difficulties arose in finding a reaction solvent in which (1) the dimers are soluble at the low reaction temperatures required to slow the reaction sufficiently to allow rates to be measured and (2) NMR peaks due to the mixed product **11** and either **9** or **10** are resolved sufficiently to be reliably integrated. Ethereal solvents such as THF satisfy only the former requirement, while aromatic solvents such as toluene only the latter. A 3:2 (by weight) toluene-d_8/THF-d_8 mixture proved to be a useful compromise: although only a relatively small range of reactant concentrations could be used due to opposing solubility and NMR sensitivity constraints, the methyl signals due to the methylcyclopentadienyl rings of **10** and **11** were well resolved (9.7 Hz separation at 200 MHz) and therefore readily monitored. Two reactions were carried out at −26 °C under pseudo-first-order conditions by using a 5-fold excess of starting dimer **9**. Good linear plots of the form shown in eq 2 were obtained to greater than 3 half-lives (Figure 2). For [**9**] = 0.04 M, $k_1 = (9.1 \pm 0.5) \times 10^{-4}$ s^{-1}, while for [**9**] = 0.012 M, $k_1 = (6.5 \pm 0.2) \times 10^{-4}$ s^{-1}. Hence, for a 3-fold drop in concentration of **9**, the rate of disappearance of **10** fell by only 30%. The data suggest, then, that the scrambling process is *not* a simple bimolecular process and could be a unimolecular process with $k_1(-26\ °C) = (8 \pm 2) \times 10^{-4}$ s^{-1}. That is, the data are consistent with the cleavage mechanism (path A) of Scheme IV. However, it must be emphasized that the data

(10) Theopold, K. H.; Bergman, R. G. *J. Am. Chem. Soc.* **1981**, *103*, 2489–2491; **1983**, *105*, 464–475.

(11) (a) Bradshaw, C. P. C.; Howman, E. J.; Turner, L. *J. Catal.* **1967**, *7*, 269–276. (b) Calderon, N.; Ofstead, E. A.; Wad, J. P.; Judy, W. A.; Scott, K. W. *J. Am. Chem. Soc.* **1968**, *90*, 4133–4140.

(12) Moore, J. W.; Pearson, R. G. "Kinetics and Mechanism", 3rd ed.; Wiley: New York, 1981; Chapter 8.

Table II. ^{1}H NMR[a,b] of 2 and 6-8

compd	CpCo	Me*Cp*Co	*Cp*CoP	Me*Cp*CoP	*Me*CpCo	*Me*CpCoP
2	4.92		4.51			
6[c]		4.81		4.49, 4.15	2.09	1.90
7	4.96			4.47, 4.14		1.89
8		4.79	4.52		2.07	

[a] C_6D_6 solution. [b] Peaks due to $PPhMe_2$ not listed. [c] See preceding paper.[8]

do not prove this mechanism, since it requires that reaction of CpCo(CO) with **9** (to give $[CpCo(CO)]_3$) or with phosphines be slow relative to dimerization. Thus, for instance, more complicated processes (perhaps involving radical chain reactions initiated by traces of $CpCo(CO)^+$) cannot be ruled out. In any case, and perhaps not surprisingly given the generally short lifetime of proposed concerted mechanisms in organometallic chemistry,[13] a simple [2 + 2] mechanism appears not to be operative.

Regardless of the mechanism of neutral dimer scrambling, access to the desired monophosphine adducts **7** and **8** is provided by this route. Thus, addition of $PPhMe_2$ to a mixture of neutral dimers **9**, **10**, and **11** gives rise to a mixture containing the four phosphine adducts **2**, **6**, **7**, and **8**. The particular phosphine used was chosen since it (as well as other alkyl phosphines such as PMe_3 and PEt_3) gives stable adducts. However, it is more easily handled than PMe_3 and gives cleaner NMR spectra than PEt_3; PPh_2Me would probably also have been a suitable choice. The ^{1}H NMR spectrum of **2** and **6–8** is shown in Figure 3a and the assignments are given in Table II. Signals due to phosphine adducts **2** and **6** are of course easily identified by independent synthesis of these adducts from dimers **9** and **10**; two features of the assignment for **6** nonetheless deserve comment. One is the singlet at δ 4.81 for the protons on the methylcyclopentadienyl ring, which presumably coincidentally all have the same chemical shift. The other concerns the assignments of the signals at δ 1.90 and 2.09 due to the two ring methyls: the broader of the two (2.5 vs. 1.3 Hz wide) at δ 1.90 is assigned to the ring on the phosphine-bearing cobalt. The assignments due to adducts **7** and **8** in the spectrum of **2** and **6–8** follow in a straightforward manner by comparison of chemical shifts and integrations. The assignments also confirm those of the two features of adduct **6** mentioned above in that the signal analogous to that of **6** at δ 4.81 appears in **8** as a multiplet at δ 4.79, while the integrations of the ring methyls when compared to those of the ring protons confirm that the high-field methyl signals (overlapping at δ 1.89 and 1.90) are on the ring on the phosphine-bearing cobalt.

Integrations of spectra of **2** and **6–8** show that the mixed compounds **7** and **8** were reproducibly formed in a 60:40 ratio. While we have been unable to determine if this preference is kinetic or thermodynamic, we note that allowing a mixture of **2** and **6–8** to stand in the presence of a 2-fold excess of $PPhMe_2$ at room temperature for 6 h results in 97% decomposition of **2**, 40% of **6**, and 60% of **7** and **8**, which nonetheless remain in a 60:40 ratio (the decomposition products are the corresponding carbonylphosphines $(\eta^5\text{-}RC_5H_4)Co(CO)PPhMe_2$, R = H, Me). On the basis of the large difference in kinetic stability between bis-Cp adduct **2** and bis-MeCp adduct **6**, it is likely that the 60:40 ratio of unsymmetrical adducts **7** to **8** is maintained by thermal equilibration (via either intra- or intermolecular phosphine exchange) and that the preference for **7** is therefore thermodynamic.

Proof of Dinuclear Elimination of *o*-Xylylene from Dimetallacycles 1 and 5. Our purpose in generating **7** and **8** lay in being able to detect these compounds in the presence of **2** and **6**, in order to determine whether any crossover as shown in Scheme II occurs. Examination of the spectra of **2** and **6–8** shows that two peaks stand out as being diagnostic for **7** and **8**. These are the singlet of **7** at δ 4.96 due to the cyclopentadienyl ring on the non-phosphine-bearing cobalt and the singlet of **8** at 2.07 for the ring methyl also on the non-phosphine-bearing cobalt. Of these, the signal at 4.96 is significantly better resolved and would be expected to provide a more sensitive test for the presence of the mixed adducts. Unfortunately, the major side product of the actual crossover experiment, *o*-xylylene spiro dimer **4b** (Scheme I), also has a signal (one of the exocyclic methylene protons) at δ 4.96. This problem was easily overcome simply by deuterating the organic moieties of the starting metallacycles **1** and **5**, by preparing them from α,α'-dibromo-*o*-xylene-d_8. The metallacycles so formed exhibited $<2.5 \pm 1\%$ residual protons in the methylene positions and, hence, could at most give rise to 0.3% residual signal at δ 4.96 from the spiro dimer.

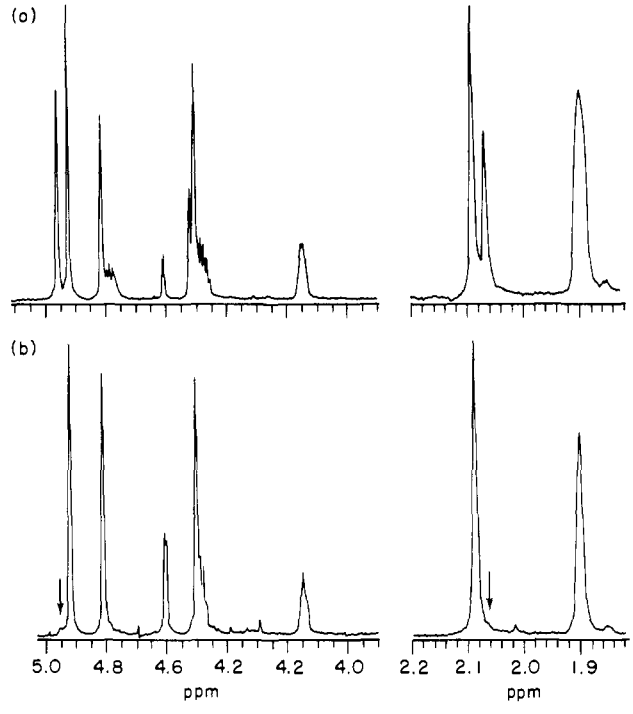

Figure 3. (a) Cyclopentadienyl and *methyl*cyclopentadienyl regions of ^{1}H NMR spectrum of **2** and **6–8**, obtained by addition of $PPhMe_2$ to a mixture of neutral dimers **9–11** prepared from **9** and **10**. (b) ^{1}H NMR spectrum of **2** and 6 obtained by addition of $PPhMe_2$ to a mixture of **1**-d_8 and **5**-d_8.

The result of mixing substituted and unsubstituted dimetallacyclohexenes **1**-d_8 and **5**-d_8, followed by addition of a 3-fold excess of $PPhMe_2$, is shown in Figure 3b. A fairly clean spectrum is obtained consisting of symmetrical phosphine adducts **2** and **6**, and the small amount of $CpCo(CO)PPhMe_2$ that is always observed due to rapid decomposition of **2**. Small residual peaks are visible at δ 4.96 and 2.07, which if they are due to mixed adducts **7** and **8** would comprise <2% of the total of **2**, **6**, **7**, and **8**. *Thus, the overall result is that the elimination of o-xylylene from 1 (and 5) is ≥98% dinuclear.* Extrusion of the organic moiety occurs from the intact dinuclear metallacycle and does not involve any cleavage of the dinuclear system before (or after) the elimination reaction. This reaction therefore represents the first conclusive evidence for dinuclear elimination that we have observed in these dicobalt systems.[5-7]

Kinetics of *o*-Xylylene Elimination. Phosphine-Induced Reaction. The next question we sought to answer in considering the reaction of benzodimetallacyclohexene **1** with phosphines concerned the detailed mechanism of the *o*-xylylene elimination. Previous kinetic studies of dinuclear cobalt systems[5b,d,e] had shown that the rate of phosphine-induced decomposition was (1) first

(13) Halpern, J. In "Organic Syntheses via Metal Carbonyls"; Wender, I., Pino, P., Eds.; Wiley: New York, 1977; Vol. II, p 705–730.

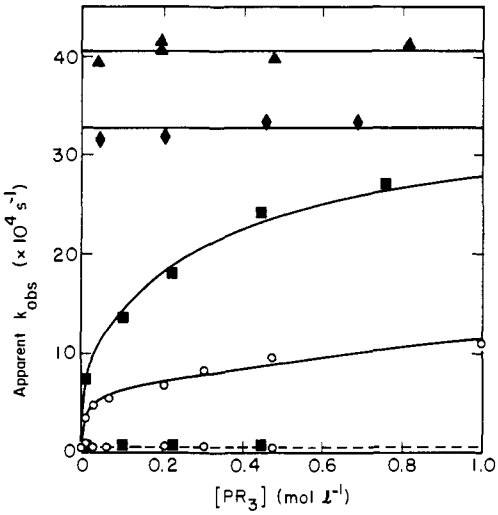

Figure 4. Dependence of the apparent pseudo-first-order rate constants (k_{obsd}) at 21.5 °C in THF-d_8 for (1) the disappearance of **1** with formation of **2**, **4**, **12**, and **13** (solid lines) and (2) the appearance of **12** and **13** (dashed line) on the concentration of PPh_3 (○), PCy_3 (■), $P(OMe)_3$ (♦), and PMe_3 (▲).

Scheme V

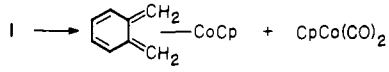

12 13

order in the dicobalt compound and (2) increased sharply as a function of phosphine concentration when the concentration was low and then leveled off to a maximum rate at high phosphine concentration. Such behavior can be readily accounted for by a mechanism in which the starting material is interconvertible with an intermediate that can be irreversibly trapped by phosphines, leading eventually (via any number of fast steps) to the final observed product. The maximum decomposition rate is simply the rate of formation of the intermediate, which at high phosphine concentration is rapidly trapped, while at low phosphine concentration the rate of return of the intermediate to starting material becomes competitive with the rate of trapping by phosphine, and hence the rate of decomposition decreases.

In order to test this type of mechanism we examined the rate of decomposition of **1** as a function of phosphine concentration for three different phosphines and one phosphite. The reactions were monitored by ^1H NMR in a probe held at 21.5 °C; the solvent was THF-d_8 since in aromatic solvents the peak being monitored—the cyclopentadienyl resonance of **1**—is coincident with the cyclopentadienyl resonance of the $CpCo(CO)PR_3$ product for both PMe_3 and PPh_3. The results are shown in Figure 4, in which the apparent pseudo-first-order rate constants for the disappearance of **1** are plotted as a function of phosphine concentration. In addition to the products already described, the thermal decomposition products **12** and **13** shown in Scheme V are also formed, at least in those reactions slow enough to allow them to build up. Their rate of formation in the reactions in which they could be detected is therefore also plotted in Figure 4.

The results can be summarized as follows: (1) Apparent pseudo-first-order decomposition of **1** was observed in all cases, following the reactions to at least 3 and in many cases 5 half-lives. (2) Qualitatively, the observed rate profiles are in agreement with the proposed mechanism, in which at low phosphine concentration rapid increases in rate are observed as the phosphine concentrations increase, and at high phosphine concentrations the rates level off. (3) The insensitivity of the rate of thermal decomposition (Scheme V) to phosphine concentration indicates that this reaction is, within the accuracy of the data, unrelated to the phosphine decomposition pathway. Since this side reaction is such a small perturbation on the main decomposition, further discussion of it will be postponed for the moment.

Scheme VI

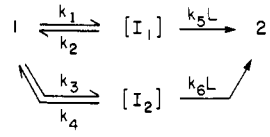

Scheme VII

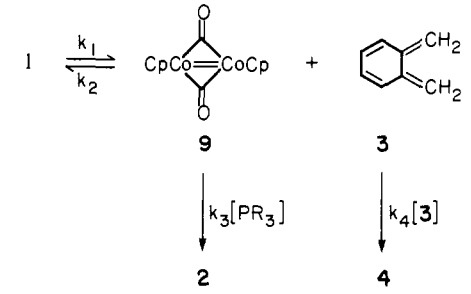

The main question these results raise is: what is the quantitative fit of the data to the mechanism under consideration? The rates fall off with differing degrees of sharpness at low phosphine concentration, indicating different rates of trapping of the intermediate interconverting with **1** by the different phosphines. In fact the falloff for both PMe_3 and $P(OMe)_3$ is too sharp to measure, but clearly at low enough values of [PMe_3] and [$P(OMe)_3$], the rates must fall off to the limiting low value, namely, the rate of thermal decomposition. The degrees of falloff indicate that the efficiency of trapping the intermediate follows the order $PMe_3 \sim P(OMe)_3 \gg PCy_3 > PPh_3$ and is apparently related both to steric and electronic characteristics of the phosphines.

In spite of this, the data fit the mechanism extremely poorly. The problem is most easily seen in the region where the rates apparently level off: each curve appears to level off at a different rate, implying four different rates of formation of the intermediate in equilibrium with **1**. This qualitative description of the poor fit of the data to the proposed mechanism is born out quantitatively,[14] and so this mechanism must be discarded. Nonetheless, the rates of both PMe_3- and $P(OMe)_3$-induced decomposition are clearly independent of phosphine concentration. This can be true for either PMe_3 or $P(OMe)_3$ only if an intermediate is in fact in equilibrium with **1**, where the rate-limiting step is the rate of formation of this intermediate and is given by the rate of the PMe_3 or $P(OMe)_3$ reaction. Since these rates differ significantly—the 20% difference is far in excess of experimental error—there must actually be two intermediates in equilibrium with **1**. On the basis of further results described below, we believe that PMe_3 is anomalous in that it is trapping a higher energy intermediate that is not trapped by any of the other phosphines. The rate of the formation of this intermediate would then be given by $k_{PMe_3} - k_{P(OMe)_3} = 8 \times 10^{-4}$ s^{-1}. We will defer discussion of this complicating reaction for the moment.

Two types of mechanisms can be proposed to reconcile the apparent contradiction between requiring that an intermediate (that is, the one that can be trapped by $P(OMe)_3$) be present and

(14) For a reaction (eq i) involving trapping by a ligand L of an intermediate B that can be formed reversibly from starting material A, if L is present in pseudo-first-order excess then the well-known double reciprocal plot of $1/k_{obsd}$ (where k_{obsd} is the observed first-order rate) vs. $1/L$ should be linear. The rate constants k_1 and k_2/k_3 can then be determined from the intercept and slope, respectively; see e.g.: Basolo, F.; Pearson, R. G. "Mechanisms of Inorganic Reactions", 2nd ed.; Wiley: New York, 1967; p 581–583. Application to the rate data for the reaction of PPh_3 and **1** gives $k_1 = (8.2 \pm 0.9) \times 10^{-4}$ s^{-1} and of PCy_3 and **1** gives $k_1 = (2.1 \pm 0.3) \times 10^{-3}$ s^{-1}. These analytically determined limiting rates bear little resemblance to observed results where $k_{obsd} = 1.1 \times 10^{-3}$ s^{-1} at 1.0 M PPh_3 and $k_{obsd} = 2.7 \times 10^{-3}$ s^{-1} at 0.8 M PCy_3. In addition to the poor fits to the data using the derived rate constants k_1 and k_2/k_3, the reciprocal plots are not linear; one measure of this is the large standard deviation in the two k_1 values so derived.

$$A \underset{k_2}{\overset{k_1}{\rightleftharpoons}} B \xrightarrow{k_3[L]} C \qquad \text{(i)}$$

Scheme VIII

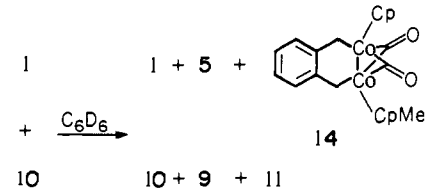

the fact that the data cannot quantitatively be fit to this single mechanism. One proposal is that there simply are two low-energy intermediates I_1 and I_2 that can be formed reversibly from starting material **1**, each capable of being trapped by phosphines at different rates to give **2** (Scheme VI). While such a mechanism does in fact provide for a quantitative fit of the data,[15] another somewhat simpler mechanism must also be considered (Scheme VII). In this mechanism starting metallacycle **1** undergoes *direct* dissociation to neutral dimer **9** and free *o*-xylylene (**3**); subsequent reaction of these two materials to give phosphine adduct **2** and organic dimer **4** would give the observed products in a straightforward manner. The rate constant k_1 for formation of the two intermediates would then correspond to the rate of $P(OMe)_3$-induced decomposition of **1**, assuming that k_4 is sufficiently large relative to k_2. Such a formation of *two* intermediates in a single pathway, as opposed to the single pathway/*single* intermediate implicitly assumed in the mechanism initially described,[14] can qualitatively account for the leveling off in rate at high phosphine concentration. Unfortunately, we do not know whether it can quantitatively account for the observed rate profiles. Even though this mechanism is the simpler of two alternatives, a cubic term appears in the steady-state rate equation due to the dimerization of *o*-xylylene, making its solution very difficult. We assume the reaction is not first order, but the NMR data are not accurate enough to establish this conclusively.

Since we did not wish to dwell on a problem that was mathematical rather than experimental in nature, we sought other ways to test the mechanism outlined in Scheme VII. The proposed mechanism itself is of fundamental interest, since in the forward direction it is analogous to a retro-Diels–Alder reaction in giving the diene *o*-xylylene and the metal–metal double-bonded species **9** and clearly in the reverse direction similarly represents a dimetalla-Diels–Alder reaction. Since we are not aware of any other examples of such a transformation, we sought independent evidence for both the forward and reverse reactions.

Scheme IX

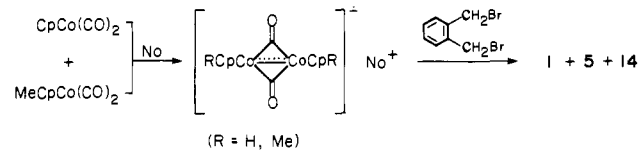

Reaction with 10. Assuming that Scheme VII in fact represents the correct mechanism, the phosphine reaction can be considered as one in which one member (neutral dimer **9**) of the pair of simultaneously generated intermediates is trapped. We therefore sought a means of trapping the other member, *o*-xylylene (**3**). Neutral dimer **9** must itself be an extremely efficient trap for *o*-xylylene, since metallacycle **1** does not decompose to **9** and dimers **4a** and **4b**; that is, **9** traps *o*-xylylene faster than the diene can dimerize. An efficient trap for *o*-xylylene, then, should be a labeled version of **9**, namely, the bis(methylcyclopentadienyl) neutral dimer **10**.

The first experiment carried out therefore involved reaction of Cp metallacycle **1** and MeCp neutral dimer **10** at room temperature in C_6D_6 (Scheme VIII). A complex mixture was obtained. ^1H NMR analysis revealed the presence of the three neutral dimers **9–11**, bis(methylcyclopentadienyl) metallacycle **5** as well as starting material **1**, and several new signals that could all be attributed to the mixed cyclopentadienyl–methylcyclopentadienyl metallacycle **14**. The identity of this material was confirmed by independent synthesis from a mixture of radical anions (Scheme IX), and the three metallacycles were readily resolved by HPLC on a reverse-phase silica column.

The formation of this complex mixture from the reaction of metallacycle **1** and neutral dimer **10** is not unexpected if it is due (Scheme X) to the trapping of free *o*-xylylene by bis-MeCp dimer **10** to give, initially, bis-MeCp dimetallacycle **5** and bis-Cp dimer **9**. Rapid scrambling of **9** and **10** to give mixed dimer **11** (Scheme III) followed by trapping of *o*-xylylene by **11** to give Cp/MeCp dimetallacycle **14** would eventually lead to an equilibrium mixture of the six observed compounds. In order to test this mechanism, in which bis-MeCp metallacycle **5** rather than mixed metallacycle **14** is proposed to be the initially formed product, the reaction was carried out using a 10-fold excess of dimer **10** (the concentration was 0.04 M) to preclude any appreciable amount of reaction of **1** with mixed dimer **11**. The reaction was conveniently followed by ^1H NMR in toluene-d_8; clean first-order disappearance of **1** ($k(-3\ °C) = (1.16 \pm 0.02) \times 10^{-4}\ s^{-1}$) to 4 half-lives was observed. The important result, however, was that at greater than 90% conversion of **1**, the specificity for formation of unmixed bis(MeCp) metallacycle **5** was greater than 93%.

Two more kinetic experiments were carried out to compare the rate of *o*-xylylene transfer to the limiting rate of phosphite-induced decomposition. Thus, in THF-d_8 at 21.5 °C, the pseudo-first-order rate constants for disappearance of **1** in 0.04 and 0.08 M **10** were $(2.8 \pm 0.1) \times 10^{-3}\ s^{-1}$ and $(2.95 \pm 0.04) \times 10^{-3}\ s^{-1}$, respectively. Thus the rates are fairly insensitive to neutral dimer concentration as would be expected on the basis of the proposed rapid trapping of *o*-xylylene by both dimers **9** and **10**. More strikingly, the rates are also in reasonable agreement with those observed in the $P(OMe)_3$ reactions, $(3.26 \pm 0.04) \times 10^{-3}\ s^{-1}$, despite the remarkably different transformations observed. Thus, the rate profile (insensitivity to neutral dimer concentration), product distribution (selective formation of metallacycle **5**), and limiting rates support the mechanisms shown in Schemes VII and X. The conclusion at this point, then, is that this unusual *o*-xylylene transfer reaction is closely related, mechanistically, to the phosphine-induced decomposition of **1**.

Reaction with Dimethyl Acetylenedicarboxylate. Although we had demonstrated, using two quite dissimilar trapping reagents, the presence of a common reaction intermediate, we still sought a system that would exhibit signs of reversibility—that is, falloff in rate at low trapping reagent concentration—but would be amenable to kinetic analysis. Ideally, such a system would involve

(15) The curves shown in Figure 4 are the theoretical least-squares best-fit lines to the data, assuming the mechanism of Scheme VI. The microscopic rate constants were determined as follows. The steady state assumption was used to give the observed rate constant k_{obsd} as a function of $k_1 - k_6$ and L, for L present in pseudo-first-order excess (eq ii). A simple linear plot that

$$k_{obsd} = \left[\frac{k_1}{(k_2/k_5) + L} + \frac{k_3}{(k_4/k_6) + L}\right]L \qquad \text{(ii)}$$

would allow an analytical determination of $k_1 - k_6$, such as that described in ref 14, cannot be derived from eq ii. A curve-fitting computer program was written to directly evaluate eq ii, by (1) using a set of arbitrary (but see below) initial guesses for the values of the rate constants to give a calculated k_{obsd} (k_{calcd}) at each value of L for each phosphine (PPh_3 and PCy_3) and then (2) numerically minimizing the function shown in eq iii with respect to each rate

$$U = (k_{obsd} - k_{calcd})^2 \qquad \text{(iii)}$$

constant. The conditions on the set of initial guesses were (1) reasonable boundaries for each rate constant and (2) $k_1 + k_3$ was assumed to be equal to the phosphine-independent (and hence limiting) rate observed for $P(OMe)_3$. The procedure was iterated until no further changes in U were observed, to give a least-squares fit of all the rate constants to all of the rate data. The thermal decomposition data can also be included in the calculation: an additional direct pathway from 1 (Scheme V) having first-order rate k_7 results in simple addition of this term to eq ii. The rate constants derived are $k_1 = 2.69 \times 10^{-3}\ s^{-1}$, $k_3 = 5.69 \times 10^{-4}\ s^{-1}$, $k_7 = 4.95 \times 10^{-5}\ s^{-1}$; PPh_3: $k_2/k_5 = 4.09$, $k_4/k_6 = 1.09 \times 10^{-2}$; PCy_3: $k_2/k_5 = 2.51 \times 10^{-1}$, $k_4/k_6 \leq 7 \times 10^{-5}$. (The upper limit on k_4/k_6 is based on the sharpest rate of falloff that we would be able to observe.) Alternatively, one could consider a pathway from either I_1 or I_2, even though this would lead to a phosphine-dependent thermal decomposition rate, in order to evaluate how the data could fit this mechanism. Nearly identical rate constants are obtained, but a much poorer fit to the rates of thermal decomposition results.

Scheme X

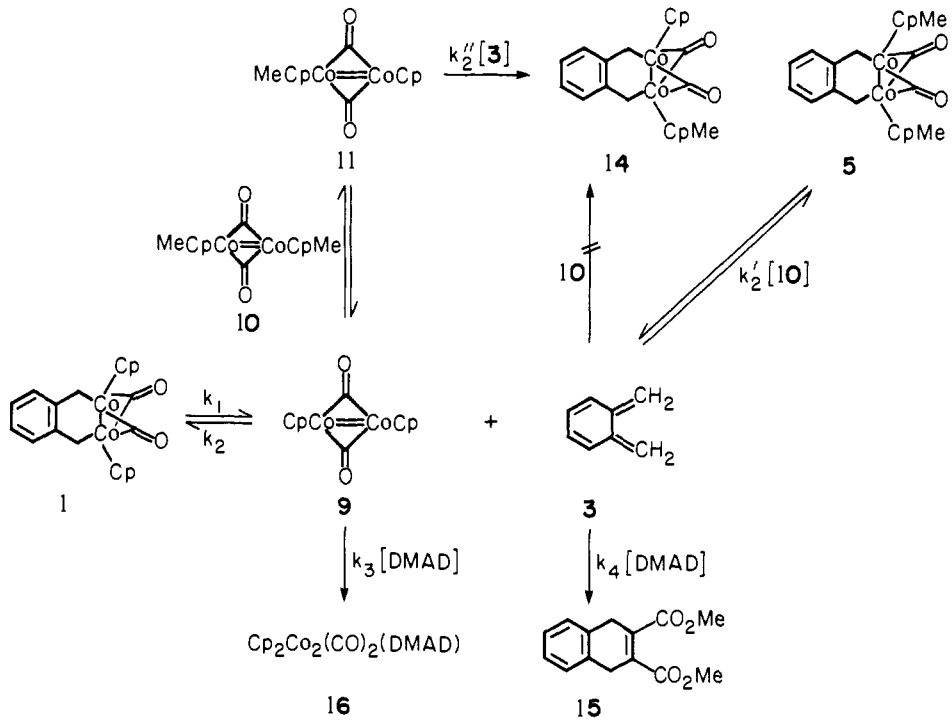

a reagent that would react with *o*-xylylene but not with neutral dimer **9**. This would allow addition of excess cobalt dimer to the reaction mixture to drive the preequilibrium toward **1** by the mass law effect; inhibition of the rate of decomposition of **1** would then serve to demonstrate that **9** was part of the bimolecular intermediate.

Unfortunately, we have been unable to find such an ideal trapping reagent. Compounds that do not react (or react slowly) at room temperature with double-bonded dimer **9**, such as unactivated olefins, acetylenes, and dienes, also do not prevent dimerization of free *o*-xylylene (generated by mercuric oxide oxidation of *N*-aminodihydroisoindole). Compounds that do prevent this dimerization, such as maleic anhydride and dimethyl acetylenedicarboxylate (DMAD), also react with **9**. Fortunately, however, we discovered that even though the steady-state analysis of the DMAD system is complex, it does yield a solution that can be compared to experimental results. We present below results that provide kinetic evidence for the presence of a reversible bimolecular reaction.

The reaction of **1** with DMAD yields the products shown in Scheme X. Addition of excess DMAD to a dark green C_6D_6 solution of **1** gives rise over the course of about 30 min to a dark red solution. The organic product has been identified by NMR as the expected *o*-xylylene DMAD Diels–Alder adduct **15**, but the detailed structure of the organometallic product **16** has not yielded to spectroscopic analysis. However, our major concern is that **16** be formed by reaction between DMAD and dimer **9** that we propose to be present in thermal equilibrium with **1**. In fact, mixing 1 equiv each of DMAD and independently prepared **9** in an NMR tube results in their complete consumption, with formation of signals identical with those assigned to **16** in the reaction of **1** with DMAD. Thus, regardless of the exact identity of **16**, it is clearly a 1:1 adduct of DMAD and **9** and presumably forms in the same manner whether the starting dinuclear material is **1** or **9**.

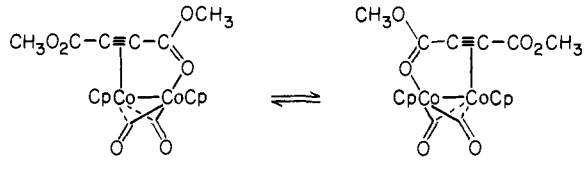

Figure 5. Suggested structure of DMAD neutral dimer adduct **16**.

Although the structure of **16** is unimportant from a mechanistic point of view, it is nevertheless of structural interest. It is easily prepared in larger quantities by reaction of **9** and DMAD in diethyl ether at room temperature. Over the course of 1 min, the reaction mixture turns color from the deep blue-green of **9** to the deep red of **16**. The speed of this reaction contrasts with that of **9** with phosphines; for instance, mixing 1×10^{-4} M solutions of **9** and PEt_3 gives an instantaneous color change from blue-green to orange, indicating complete conversion to $Cp_2Co_2(CO)_2PEt_3$ and $CpCo(CO)PEt_3$. Solvent removal followed by crystallization from ether gives **16** in low yield as black, air-stable crystals that were, unfortunately, not suitable for characterization by X-ray diffraction. ^1H NMR shows that the complex has two distinguishable cyclopentadienyl and two carbomethoxy groups, which exchange slowly on the NMR time scale at room temperature. Infrared spectra indicate the presence of bridging carbonyls, but a strong sharp band at 1989 cm^{-1} (KBr; solution spectra are similar) may be assigned as either a terminal CO or an acetylene stretching band.[16] A structure such as that shown in Figure 5 can account for the data, but the unusual nature of the bonding suggests that an X-ray crystal structure will be needed to fully characterize this material. In addition, **16** is thermally unstable, decomposing to give more uncharacterized products (the major one has two singlets corresponding to Cp and carbomethoxy moieties). Finally, the bis(methylcyclopentadienyl) analogue of **16** is readily prepared as analytically pure black air-stable needles in 76% yield. While it is somewhat more thermally stable than **16**, it too has failed to yield crystals suitable for X-ray analysis.

The kinetics of the reaction between **1** and DMAD were initially examined by ^1H NMR spectroscopy. The reactions were run under conditions analogous to those used previously for the phosphine and neutral dimer kinetics (THF-d_8 at 21.5 °C) in the presence of a large excess of DMAD. As in the previous reactions, first-order decomposition of **1** was observed to greater than 3 half-lives, but for the first time the rate profile as a function of reactant concentration (in this case DMAD) exhibited a well-behaved sharp falloff in rate at low DMAD concentration and a clear leveling off at high DMAD concentration (Figure 6). The limiting rate, 3.1×10^{-3} s^{-1}, is in excellent agreement with the

(16) Bailey, W. I., Jr.; Chisholm, M. H.; Cotton, F. A.; Rankel, L. A. *J. Am. Chem. Soc.* **1978**, *100*, 5764–5773.

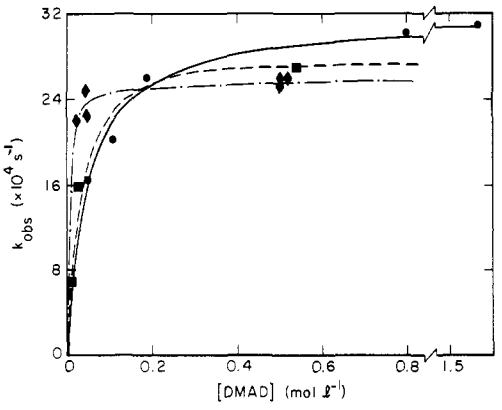

Figure 6. Dependence of disappearance of **1**, plotted as the pseudo-first-order rate constants (k_{obsd}), on DMAD concentration, for different initial concentrations of **1**. ^{1}H NMR data (21.5 °C, THF-d_8) (—) $[\mathbf{1}]_0 = 5 \times 10^{-3}$ to 5×10^{-2} M; UV–vis data (21.7 °C, THF) (---) $[\mathbf{1}]_0 = 1 \times 10^{-3}$ M; (·····) $[\mathbf{1}]_0 = 5.5 \times 10^{-5}$ M.

previous data for the value of the limiting rate of decomposition of **1** induced by both $P(OMe)_3$ and bis-MeCp doubly bonded dimer **10**. The rate data therefore again suggest the presence of an intermediate in thermal equilibrium with **1**. If Scheme X applies, at high DMAD concentration, bis-Cp doubly bonded dimer **9** and *o*-xylylene are formed in the rate-determining step and are trapped essentially every time they are formed. At low DMAD concentration, reversion back to **1** is competitive with trapping by DMAD, and a falloff in rate is observed.

This description is however incomplete. In systems that are frequently encountered involving a *single* reversibly formed reaction intermediate, both trapping to give products and reversion to starting material are first order in the intermediate, and hence the overall reaction is first order in starting material. This is not the case in a system involving reversible starting material cleavage to give two reaction intermediates—a "bimolecular intermediate". Here, trapping one of the intermediates to give products will be first order in the intermediate, while reversion to starting material will be second order. In other words, as the reaction proceeds the rate of trapping by an external ligand present in "pseudo-first-order excess" relative to the rate of trapping by the second reaction intermediate will rise as the starting material (and hence the second reaction intermediate) concentration falls. Since to a first approximation the intermediates' concentrations are proportional to the square root of the starting material concentration, the rate of the back reaction relative to the rate of the trapping reaction will fall roughly as the square root of the starting material concentration. However, only when the back reaction is competitive with the trapping reaction is falloff in the rate of starting material decomposition observed. Therefore, in terms of experimentally observable rates, the rate of falloff in the rate of starting material decomposition will decrease as the starting material concentration falls. In other words, *regardless of DMAD concentration, the rate of decomposition of* **1** *will rise to the maximum limiting rate given by* k_1 *as the concentration of* **1** *falls.*

One may therefore predict that given the mechanism shown in Scheme X, the decomposition of **1** will (1) not be first order and (2), even under conditions of low DMAD concentrations where apparent falloff in rate is observed, as [**1**] falls the rate of decomposition should increase. Under the sensitivity constraints of ^{1}H NMR, this rise in rate was not observed before **1** itself disappeared, nor was any nonlinearity in the reaction rate detected. Quantitatively, then, under what conditions will these rate behaviors be observed?

Applying the steady-state approximation to either *o*-xylylene (**3**) or dimer **9** in Scheme X and solving the resulting quadratic equation gives rise in a straightforward (if cumbersome) manner to the rate law shown in eq 3 (L = [DMAD]). It can be seen

$$\frac{-\mathrm{d}[\mathbf{1}]}{\mathrm{d}t} = \left[\frac{2k_1L}{(L^2 + [(4k_1k_2)/(k_3k_4)][\mathbf{1}])^{1/2} + L}\right][\mathbf{1}] \quad (3)$$

Table III. Rate Constants for Reaction of Complex I with DMAD

[DMAD], M	[**1**] $\times 10^5$, M	$k_{obsd} \times 10^3$, s^{-1}
0.025	5.5	2.21 ± 0.01
0.050	5.7 ± 0.1	2.6 ± 0.1[a]
0.51 ± 0.01	5.5 ± 0.1	2.58 ± 0.03[b]
0.01	120	0.67 ± 0.01
0.03	100	1.58 ± 0.01
0.54	120	2.69 ± 0.01

[a] Average of two runs. [b] Average of three runs.

that for $L^2 \gg [(4k_1k_2)/(k_3k_4)][\mathbf{1}]_o$, eq 3 reduces to a simple first-order rate law, with the limiting rate of decomposition of **1** given by k_1. Thus under conditions where [DMAD] is high enough to give the limiting rate, the reaction is in fact first order. In order to assess the behavior of eq 3 under other conditions, it was first integrated (eq 4)—again a straightforward but cumbersome process—and then numerically evaluated. In evaluating eq 4, k_1 is known and constant, and values of [**1**] and L are known for several reactions. It is necessary then to vary only $k_2/(k_3k_4)$ to determine if the experimental data can be fit to the equation. This was accomplished by adjusting $k_2/(k_3k_4)$ until the slope of the line generated by the left-hand side of eq 4 was roughly equal to the known value of $k_1 = 3.1 \times 10^{-3}$ s^{-1} and gave $k_2/(k_3k_4) = 1710 \pm 40$. Using this result, the following prediction can be made: even though 0.05 M DMAD and 0.0047 M [**1**] gave $k_{obsd} = 1.65 \times 10^{-3}$ s^{-1}, lowering [**1**] to 0.0001 M should result in $k_{obsd} = 3 \times 10^{-3}$ s^{-1}! A further drop to 5×10^{-5} M **1** will essentially result in decomposition at the limiting k_1, *even though [DMAD] is unchanged.* Thus, in accord with the qualitative description given above, the quantitative theoretical prediction given the mechanism of Scheme X is that a drop in concentration of [**1**] by roughly 2 orders of magnitude will result in a doubling of the decomposition reaction rate to the limiting value of k_1. A test of this prediction was carried out by monitoring the DMAD reaction by UV–visible spectroscopy.

$$\frac{1}{2}\left[\ln [\mathbf{1}] + \ln\left(\frac{A_t - L}{A_t + L}\right)\right] + \frac{A_t}{L} = -k_1t + C \quad (4)$$

$$A_t = \left[L^2 + 4k_1\left(\frac{k_2}{k_3k_4}\right)[\mathbf{1}]\right]^{1/2}$$

$$C = \frac{1}{2}\left[\ln [\mathbf{1}]_{t=0} + \ln\left(\frac{A_{t=0} - L}{A_{t=0} + L}\right)\right] + \frac{A_{t=0}}{L}$$

$$L = [\mathrm{DMAD}]$$

UV–Visible Kinetic Study of DMAD Reaction of 1. In order to be able to examine the reaction of **1** both as a function of [**1**] and of [DMAD], it was necessary to be able to monitor [**1**] by the same technique at widely differing concentrations. In THF at room temperature **1** exhibits (among other peaks) two absorbances in the UV–visible spectrum at 344 and 662 nm, having extinction coefficients of 17 000 and 1000, respectively. Both peaks decay upon reaction with DMAD, and hence the desired comparison was achieved by monitoring at 344 nm for low concentration decompositions of **1** and at 662 nm (in practice 700 nm was used to give absorbance readings of less than 1.0) for high concentration decompositions. The reactions were carried out under conditions similar to those of the NMR kinetics, at 21.7 ± 0.1 °C in THF, and were all followed to at least 4 half-lives. The results are collected in Table III, where the rates given are the "pseudo" pseudo-first-order rate constants, and the data are plotted in Figure 6. Several conclusions can be drawn from these data. (1) The rate profile at high $[\mathbf{1}]_0$ is in good agreement with the NMR results, in which $[\mathbf{1}]_0$ varied from 0.005–0.05 M, as opposed to 0.001 M in the UV experiments. (2) The limiting value of k_1 from the UV experiments, 2.7×10^{-3} s^{-1}, compares favorably with the NMR value of 3.1×10^{-3} s^{-1}, showing that the reaction being followed is the same. (3) The decomposition rate is highly dependent on $[\mathbf{1}]_0$, for instance falling from 2.2×10^{-3} s^{-1} when $[\mathbf{1}]_0 = 5.5 \times 10^{-5}$ M to about 1.6×10^{-3} s^{-1} (a drop of 30%) when

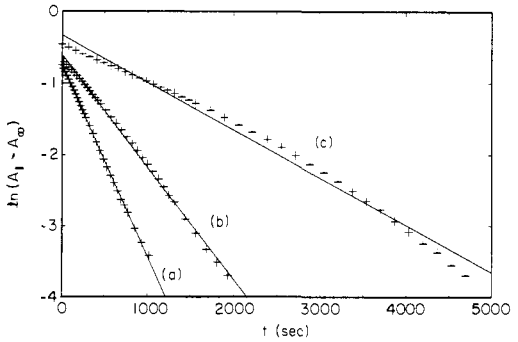

Figure 7. First-order plot of disappearance of **1** against time for $[\mathbf{1}]_0 = 1 \times 10^{-3}$ M for different (excess) concentrations of DMAD. The lines depicted are the least-squares best fits to all of the points plotted: (a) [DMAD] = 0.54 M; (b) [DMAD] = 0.03 M; (c) [DMAD] = 0.01 M.

$[\mathbf{1}]_0 = 1 \times 10^{-3}$ M, for [DMAD] $\approx$ 0.03 M. (4) At low $[\mathbf{1}]_0$, the rate is insensitive to [DMAD], since $k_{obsd} = 2.6 \times 10^{-3}$ s^{-1} for [DMAD] = 0.05–0.5 M. *The results therefore completely confirm the prediction that at low [DMAD], simply lowering the concentration of* **1** *will result in a sharp rise in its rate of decomposition.*

Two final points remain to be considered. First is the question of the linearity of the "pseudo" pseudo-first-order plots. The UV data are far more precise than the NMR data. Thus, simple examination of the high-concentration (of **1**) plots of ln $(A_t - A_\infty)$ vs. time provides a striking demonstration of the dependence of rate on [**1**] (Figure 7). At the lowest concentration of DMAD (0.01 M), the curvature is pronounced, giving an initial rate of 5.2×10^{-4} s^{-1} as compared to the overall rate of 6.7×10^{-4} s^{-1}. At [DMAD] = 0.03 M, the curvature is less severe, but even so the initial rate is significantly slower (1.25×10^{-3} s^{-1}) than the overall rate of 1.6×10^{-3} s^{-1}. In fact, in comparing this result to that where [**1**] = 5.5×10^{-5} M (point 3 above) it is clear that this lower rate provides the proper comparison: *the decomposition rate upon lowering* $[\mathbf{1}]_0$ *from* 1×10^{-3} *to* 5.5×10^{-5} *M rises by nearly 2-fold, from* 1.25×10^{-3} *s*$^{-1}$ *to* 2.2×10^{-3} *s*$^{-1}$. Finally, as seen in Figure 7, at [DMAD] = 0.5 M a good linear plot is obtained, since the limiting rate has been achieved at this concentration of trapping reagent.

The second point concerns the value of $k_2/(k_3k_4)$. From eq 3, and if $L^2 \ll [(4k_1k_2)/(k_3k_4)][\mathbf{1}]$, then the overall rate law reduces to eq 5, and the integrated rate law to eq 6. This condition

$$-\mathrm{d}[\mathbf{1}]/\mathrm{d}t = L[(k_1k_3k_4[\mathbf{1}])/k_2]^{1/2} \quad (5)$$

$$[\mathbf{1}]^{1/2} = (-L/2)[(k_1k_3k_4)/k_2]^{1/2}t + [\mathbf{1}]_0^{1/2} \quad (6)$$

appears to be fulfilled for the two kinetic runs where [DMAD] is low and $[\mathbf{1}]_0$ is high, that is the two "curved" plots. Thus, plotting $(A_t - A_\infty)^{1/2}$ vs. time for the first half-life (where [**1**] remains sufficiently high) gave excellent straight lines from which were derived $k_2/(k_3k_4)$ = 1250 ± 90 and 1850 ± 130 for the [DMAD] = 0.01 and 0.03 M runs, respectively. The large standard deviations reported are due to uncertainty in the extinction coefficient, not in the lines themselves. Application of the procedure used for the NMR data (see eq 4) gave $k_2/(k_3k_4)$ = 1790 ± 70. In any case, the value of 1550 ± 300 derived from eq 6 is in reasonable agreement with that derived from the NMR data, especially given that the k_1 values also differ slightly.

While the relative constancy of $k_2/(k_3k_4)$ is important in determining whether the theoretical results are consistent with the experimental data, its actual value is also of importance: if we can approximate k_3 and k_4, then k_2, the rate of the forward dimetalla-Diels–Alder reaction, can be determined. The rate of reaction of dimer **9** and DMAD is fairly slow for an "intermediate"; as described above the reaction takes 30–60 s at room temperature. If we assume that (1) that is the time for roughly 90% reaction and (2) the reaction is second order, then given the known reactant concentrations we can estimate that k_3 is roughly 10 M^{-1} s^{-1}. In order to approximate k_4, we know that DMAD prevents *o*-xylylene dimerization, and hence k_4[DMAD][**3**] $\gg k_5[\mathbf{3}]^2$, where k_5 is the rate constant for *o*-xylylene dimerization. While this rate constant has been measured,[17] the reported product was 1,5-dibenzocyclooctadiene (**4a**) rather than **4b**, the usual product of room-temperature dimerization of *o*-xylylene.[18] Nevertheless, since it is the only estimate available, we will assume $k_5 = 1 \times 10^4$ M^{-1} s^{-1}. Using the steady-state approximation from which eq 3 was derived, [**3**] can be approximated for given values of [DMAD] and $[\mathbf{1}]_0$ as a function of k_4. For instance, using the NMR values for [DMAD] = 0.05 M and $[\mathbf{1}]_0$ = 0.0047 M gives [**3**] = $(8 \times 10^{-5})/k_4$ M, and hence, using the fact that DMAD prevents dimerization of **3**, $k_4 \gg 4$ M^{-1} s^{-1}. Thus, since $k_2 \approx 1550k_3k_4$, the lowest estimate of k_2 is on the order of 6×10^4 M^{-1} s^{-1}. Hence the rate constant for reaction of *o*-xylylene with **9** is on the order of 10 times greater than its rate constant for dimerization, and thus the rate of the forward dimetalla-Diels–Alder reaction is indeed quite rapid.

In conclusion, then, the kinetic data are in excellent qualitative and quantitative agreement with a mechanism (Scheme X) involving reversible equilibration of dimetallacycle **1**—in a single pathway—with two reactive intermediates, *o*-xylylene (**3**) and dimer **9**, each of which is trapped by DMAD. The mechanism is in effect a dimetalla-retro-Diels–Alder reaction. Since such a reaction is without precedent, we sought both to characterize it somewhat more fully energetically and also to examine the forward ring-forming reaction in a preparative manner.

Activation Parameters for the Retro-Dimetalla-Diels–Alder Reaction. In order to obtain accurate activation parameters for the cleavage of **1** to **3** and **9**, the reaction was examined again by UV spectroscopy. In principle any ligand that assures disappearance of **1** at the limiting maximum rate may be used; in that case the desired activation parameters are simply those associated with the cleavage rate constant k_1. The obvious candidate is DMAD, because this is the ligand for which kinetic proof of the bimolecular nature of the intermediate exists. However, it undergoes a secondary reaction: catalytic cyclotrimerization of DMAD, possibly via DMAD adduct **16**, occurs, and while this in no way affects the room-temperature kinetics described above, it does give rise to end-point problems in the high-temperature reactions needed for an Arrhenius plot. For this reason, $P(OMe)_3$ was used instead, since the reaction proceeds directly, without observable intermediates, from **1** to the final product $CpCo(CO)P(OMe)_3$.

Several reactions were carried out to ensure that $P(OMe)_3$ was a suitable choice for this study. At 21.6 °C in THF, using (5.6 ± 0.1) × 10^{-5} M **1**, 0.05 M $P(OMe)_3$ gave k_{obsd} = (2.70 ± 0.03) × 10^{-3} s^{-1}, while 0.52 M $P(OMe)_3$ gave k_{obsd} = (2.735 ± 0.005) × 10^{-3} s^{-1}, in good agreement with the DMAD data. Three reactions at 26.6 °C at $[P(OMe)_3]$ = 0.05, 0.49, and 1.48 M gave $k_{obsd} = 5.50 \times 10^{-3}$, 5.63×10^{-3}, and 5.90×10^{-3} s^{-1}, respectively. The slight increase in rate may be due either to solvent effects or to a closer approach to saturation behavior. Since saturation behavior—that is, measurement of the limiting rate—was desired, the reactions were carried out using 1.5 M $P(OMe)_3$. Thus, a plot of ln (k/T) vs. $1/T$ for seven reactions of **1** with $P(OMe)_3$ carried out from 2.6 to 36.8 °C gave $\Delta H^\ddagger$ = 24.3 ± 0.4 kcal/mol and $\Delta S^\ddagger$ = +12.1 ± 1.2 eu. The positive entropy is in accord with the proposed mechanism, given similar values in organic retro-Diels–Alder reactions.[19]

Direct Reaction between 3 and 9. The final proof sought for the mechanism in Scheme X was to show that direct reaction of *o*-xylylene and neutral dimer **9** would give rise to metallacycle **1**. It is of course not possible to generate substantial concentrations of *o*-xylylene in solution, but generation as a transient intermediate from suitable precursors is well-known. Our requirements for these precursors were (1) low temperature generation, because **1** is thermally sensitive, and (2) nonoxidative (or only mildly so) generation, as **9** is readily oxidized. Two methods that were

(17) Roth, W. R.; Biermann, M.; Dekner, H.; Jochems, R.; Mosselman, C.; Hermann, H. *Chem. Ber.* **1978**, *111*, 3892–3903.
(18) Errede, L. A. *J. Am. Chem. Soc.* **1961**, *83*, 949–954.
(19) Benson, S. W.; O'Neal, H. E. "Kinetic Data on Gas Phase Unimolecular Reactions"; National Bureau of Standards: Washington, D.C., 1970.

Scheme XI

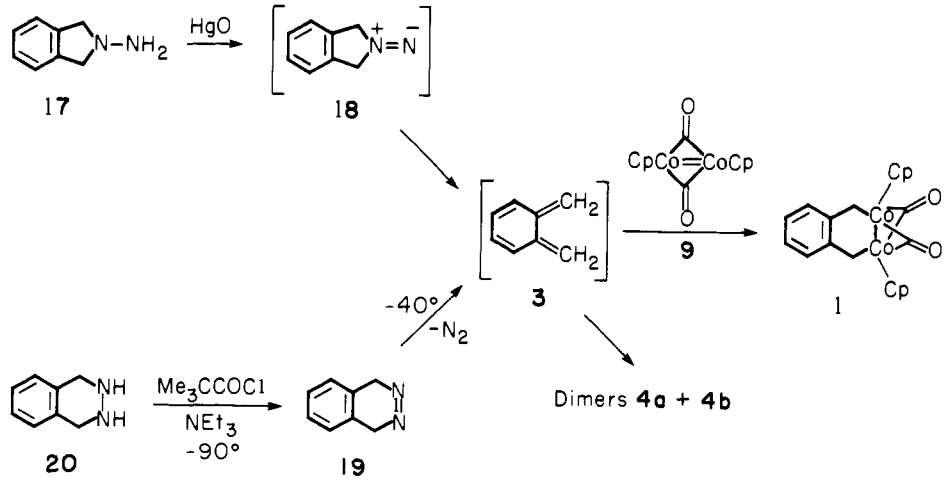

successfully employed are described below.

The first precursor used was *N*-aminodihydroisoindole (**17**, Scheme XI), which at room temperature in C_6D_6 solution is slowly (about 20 min) oxidized by brown mercuric oxide to give dimers **4a** and **4b**.[20] The reaction presumably proceeds via the thermally (even, presumably, at −78 °C) unstable 1,1-diazine[21] **18** to give free *o*-xylylene. Repetition of this reaction under identical conditions but now in the presence of 1 equiv of dimer **9** gave rise to a mixture of products. In this mixture, *22% of the ^1H NMR cyclopentadienyl intensity was due to* ***1***; singlets of the appropriate intensity at δ 7.04 and 1.70 due to the aromatic and methylene protons confirmed the identity of the Cp at 4.56 as being due to **1**. The other products included $CpCo(CO)_2$ (and possibly unresolved **9**) at δ 4.39 (56%), $[CpCo(CO)]_3$ at 4.62 (12%), and an unidentified cyclopentadienyl peak at 4.58 (10%). *Just as important as the observation of* ***1*** *was the fact that no o-xylylene dimer* ***4*** *was observed*; greater than 4 mol % (relative to the Cp-containing products) would have been detected. The result of this experiment, then, is that cobalt dimer **9** completely inhibits dimerization of *o*-xylylene, and that roughly 20% of the products of this inhibition give dimetallacycle **1**.

We next sought the use of a precursor that would avoid the presence of an oxidizing reagent in the presence of dimer **9** and product **1**. While the 1,1-diazine **18** generated from hydrazine **17** is not isolable, 1,4-dihydrophthalazine[22] (**19**), prepared from the isomeric hydrazine **20**, is stable at low temperatures. Warming to roughly −40 °C leads to slow evolution of nitrogen with formation of organic dimer **4b**, presumably through the intermediacy of *o*-xylylene. Such a thermal reaction is ideal for the purpose at hand, and therefore several reactions of cobalt dimer **9** with azo compound **19** were carried out.

The reaction was first carried out on a small preparative scale by addition of *tert*-butyl hypochlorite to a stirred THF solution of hydrazine **20** and triethylamine at −90 °C, to generate **19**. A cold THF solution of **9** was then added, and the mixture was allowed to rapidly warm to room temperature. A gradual color change from the deep blue-green color of **9** to the olive-green color of **1** was observed. Solvent removal was followed by extraction of the residue with C_6D_6 and addition of ferrocene as an internal NMR standard. A remarkably clean NMR spectrum was obtained, in which 81% of the cyclopentadienyl intensity was due to dimetallacycle **1**, 16% to $CpCo(CO)_2$ (and possibly unresolved **9**), and 3% to $[CpCo(CO)]_3$. On the basis of the internal standard, the recovery of Cp-containing products was 53%, and the absolute yield of **1** (based on hydrazine **20**) was 45%. In accord with the NMR results, column chromatography of this mixture yielded 5 mg of **1**, an isolated yield of 34%. In addition to the isolation of **1**, this experiment gave one other important result: on the basis of the NMR spectrum of the reaction mixture, <3 mol % of the *o*-xylylene dimer **4b** was present. *Thus, once again, reaction of an o-xylylene precursor and neutral dimer* ***9*** *led to formation of* ***1*** *with complete inhibition of o-xylylene dimerization.*

Attempts to monitor this reaction by NMR were less successful. Conversion of **9** and **19** was observed, but additional (unidentified) products were also formed; the extent of diversion to these other products seemed to depend both on concentration and temperature. It is our guess that some *direct* reaction occurs between azo compound **19** and dimer **9**, in competition with nitrogen extrusion to give *o*-xylylene. The nitrogen extrusion reaction of **19** has an activation entropy of -7 ± 2.5 eu;[22] it would be expected that the direct bimolecular reaction would have a much more negative entropy. Thus, raising the reaction temperature would give relatively more nitrogen extrusion and hence formation of **1**, as observed. In addition, formation of **1** was observed only at a temperature where thermal decomposition of **19** is known to occur, even though the rate of decomposition was somewhat more rapid than expected. While the complexity of the system precludes quantitative kinetic analysis (i.e., to show that the reaction to form **1** is first order in azo compound precursor and zero order in dimer **9**), we suggest that the weight of the evidence favors a mechanism involving thermal loss of nitrogen to give *o*-xylylene, followed by trapping by dimer **9** to give **1**. Furthermore, the fact that formation of **1** is observed in the reaction of **9** with two *different* *o*-xylylene precursors is perhaps the best evidence that a dimetalla-diels–Alder reaction has occurred.

Mechanism of Thermal Decomposition. We return briefly to one final point on which discussion had been deferred, namely, the mechanism of thermal decomposition of dimetallacycle **1** to mononuclear *o*-xylylene complex **12** and $CpCo(CO)_2$ (**13**) (Scheme V). In the absence of trapping agents such as phosphines or DMAD, the reaction proceeds slowly and quantitatively with a first-order rate constant $k = (3.8 \pm 0.2) \times 10^{-5}$ s^{-1} at 21.5 °C in THF-d_8. The thermal products **12** and **13** could also be detected as minor products in most of the decompositions of **1** by PPh_3 and PCy_3. With $[PR_3] \gg [\mathbf{1}]_0$, the two decomposition pathways are first order, the reactions are parallel, and the rate constants are therefore simply proportional to the extents of reaction along each pathway. Thus, the rate of formation of the thermal products for each reaction was calculated as a fraction of the overall decomposition rate, by measuring the final concentrations of **12**, **13**, and $CpCo(CO)PR_3$. For the reactions in which **12** and **13** were detected an average value of $k = (4.5 \pm 0.3) \times 10^{-5}$ s^{-1} was found, in reasonable agreement with the directly determined value.

The lack of dependence of the rate of thermal decomposition on phosphine concentration suggests that a common intermediate cannot be involved in these two reactions. Since the phosphine-induced reaction involves reversible loss of *o*-xylylene, this suggests that the thermal reaction is intramolecular. In principle one can test this hypothesis via a double-laeling experiment, in which for

(20) Carpino, L. A. *J. Am. Chem. Soc.* **1962**, *84*, 2196–2201.
(21) Hinsberg, W. D., III; Schultz, P. G.; Dervan, P. B. *J. Am. Chem. Soc.* **1982**, *104*, 766–773.
(22) Flynn, C. R.; Michl, J. *J. Am.* Chem. *Soc.* **1974**, *96*, 3280–3288.

Scheme XII

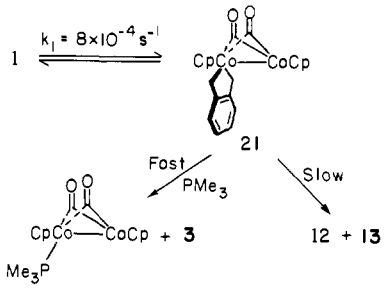

instance deuterated bis-Cp dimetallacycle **1**-d_8 (where the *o*-xylylene moiety is completely deuterated) and unlabeled bis-MeCp dimetallacycle **5**-d_0 are mixed and allowed to thermally decompose; any crossover—that is intermolecular reaction—would be evidenced by the presence of undeuterated mononuclear *o*-xylylene complex **12**. Of course such an experiment will fail if scrambling of the label in the starting material is observed, as is in fact the case. Thus, mixing deuterium-labeled bis-Cp dimetallacycle **1**-d_8 and its unlabeled bis-MeCp analogue **5**-d_0 gives within 15 min (before any significant thermal decomposition can occur) a completely scrambled mixture of protio- and deuterio-**1** and **5**. This result is of course not unexpected and provides further evidence for the complete dissociation of **1** and **5** into *o*-xylylene and neutral dimers **9** and **10** which interchange CpCoCO fragments, as established earlier.

There is one other piece of evidence that may be relevant to the mechanism of thermal decomposition. As described above, the rates of both PMe_3- and $P(OMe)_3$-induced decomposition of **1** are independent of ligand concentration, yet they differ by 20%. We suggested that $P(OMe)_3$ reacts with doubly bonded dimer **9** at the limiting rate and that PMe_3 traps, in addition to this, a higher energy intermediate. The rate of that trapping would then be just the difference in the two overall rates, $(7.9 \pm 0.6) \times 10^{-4}$ s^{-1}. In order that the number of proposed independent reaction pathways available to **1** not proliferate too greatly, we suggest that this intermediate is on the thermal decomposition pathway, and that the high nucleophilicity of PMe_3 is responsible for the fact that it alone can trap this high-energy intermediate. Since this rate of 8×10^{-4} s^{-1} is higher than the rate of thermal decomposition, there must be an additional barrier to thermal decomposition that is the actual rate determining step. A mechanism may be proposed (Scheme XII) in which reversible alkyl transfer from one cobalt to the other results in an intermediate (**21**) that is similar to the dinuclear monophosphine adducts. Attack of phosphine (at either cobalt) would then give the products in a straightforward manner, while cleavage to give **12** and **13** would seem to be a similarly energetically feasible process. Detection of the rearrangement implied by this equilibrium should be possible with a suitably labeled version of **1**, but this has not yet been attempted. The mechanism is attractive in that evidence for reversible alkyl transfer exists in a dicobalt dimethyl system[23] and in that evidence for a dinuclear phosphine-trappable intermediate exists in a dicobaltacyclopentane system.[5d,e] To the extent that the mechanisms of dicobaltacycle decompositions should be similar, such a mechanism provides a link between the seemingly dissimilar chemistries of the saturated five-membered system and the partly unsaturated six-membered **1**. The difference, of course, is that intermediate **21** (and hence **1**) has a low-energy decomposition pathway available to it that involves only cobalt–cobalt bond cleavage and rearrangement of σ- to π-bound *o*-xylylene, while no such similar low-energy pathway exists for a saturated system.

Conclusion

We have reported a detailed study of a variety of reactions of the first dimetallacyclohexene. All evidence strongly supports a mechanism in which the predominant reaction pathway involves reversible cleavage of the dimetallacycle in Diels–Alder fashion to give a metal–metal double-bonded compound and the reactive diene *o*-xylylene. This evidence can be summarized as follows: (1) Crossover experiments demonstrated that the loss of *o*-xylylene from starting dimetallacycle **1** in its reactions with phosphines to give monophosphine adduct **2** is a dinuclear elimination process that leaves the cobalt–cobalt bond intact. (2) Kinetic studies showed that the reactions with phosphines proceed by trapping a reactive intermediate that is in thermal equilibrium with **1**. (3) Reaction of **1** with the bis(methylcyclopentadienyl) neutral dimer **10** resulted in *o*-xylylene transfer from one intact dicobalt moiety to another. (4) The rate study of this *o*-xylylene transfer reaction indicated that it proceeds via the same intermediate postulated in the phosphine reactions. (5) Rate studies of the reaction of **1** with dimethyl acetylenedicarboxylate (DMAD) showed that it too proceeds via the same reaction intermediate, and the products were those formed individually by reaction of DMAD with neutral dimer **9** and with *o*-xylylene (**3**). (6) On the basis of the assumption that **1** was therefore in thermal equilibrium with *two* reactive intermediates (neutral dimer **9** and *o*-xylylene), the prediction was made that the falloff in decomposition rate of **1** at low DMAD concentration could be eliminated by simply lowering the concentration of **1**. Experimental confirmation of this key prediction provided the first kinetic evidence in this study that was both consistent with the observation of a reversible dimetalla-Diels–Alder reaction and completely inconsistent with any mechanism involving a single reaction intermediate. (7) Reactions between two different *o*-xylylene precursors and neutral dimer **9** both gave dimetallacycle **1**, providing the first preparative evidence that the direct dimetalla-Diels–Alder reaction had in fact been observed. We were, however, unable to obtain definitive kinetic and/or spectroscopic evidence that might rule out non-Diels–Alder type mechanisms for the formation of **1** in those two reactions. (8) Finally, the equilibrium proposed to exist between **1** and **9** and *o*-xylylene is particularly remarkable in that *o*-xylylene dimerization to **4** was not observed in the absence of reagents that react with **9**; in other words, thermal decomposition of **1** to **9** and **4** was not observed. In accord with this fact, no *o*-xylylene dimer **4** was detected in the reactions between the *o*-xylylene precursors and excess **9**. Hence, the cycloaddition reaction between double-bonded cobalt dimers and *o*-xylylene must be a remarkably rapid process.

While most of the data can be accounted for by the postulated dimetalla-Diels–Alder reaction, some of the results suggested the presence of another, albeit minor, reaction pathway. Thus, thermal decomposition of **1** to the two mononuclear compounds **12** and **13** appeared to be unaffected by the phosphine reaction in which one of the two reactive intermediates in equilibrium with **1** was trapped and hence removed from the equilibrium. In addition, PMe_3 apparently trapped another intermediate in equilibrium with **1** in addition to reacting via the predominant retro-Diels–Alder pathway. These results can be accommodated by a second reaction pathway that may be analogous to that observed in other dicobalt systems.

The possibility that the second reaction pathway exists is satisfying in that it suggests a common mechanistic thread may exist to tie it together with a variety of seemingly unrelated reactions.[5,6] In comparing the reactions of **1** with those of other dimetallacycles, the dissimilarity may readily be related to the facile conversion of the organic moiety to *o*-xylylene. Clearly, a low-energy reaction pathway exists involving this conversion along the retro-Diels–Alder pathway. However, this facile rearrangement also occurs along the independent higher energy pathway, giving *o*-xylylene trapped in the form of a mononuclear complex. This type of rearrangement cannot occur in the other dicobalt complexes, and hence different chemistry ensues.

In conclusion, then, our results demonstrate that thermal equilibration of a dimetallacyclohexene with a dimetallaolefin and diene can be a remarkably facile process. We began this study, in part, in order to examine the thesis that reactions at two metal centers may give rise to chemistry without analogy in mononuclear systems. The observation of this novel ring-forming and -breaking reaction, the first such demonstration of a dimetalla-Diels–Alder

(23) Matturro, M. G.; Bergman, R. G., unpublished results.

reaction, suggests that thesis is correct.

Experimental Section

General. The methods and instruments used, except as noted here, are identical with those described in the preceding paper.[8] The ^{1}H NMR spectra were all recorded at 200 or 250 MHz.[8] Chemical ionization mass spectra were obtained on a Finnegan 4000 spectrometer using methane gas. Ultraviolet–visible spectra were recorded on a Hewlett-Packard 8450A UV–visible spectrophotometer. Kinetic spectrophotometric analyses were carried out with a Carey 118 spectrophotometer driven by a Carey 1818 digital repetitive scan accessory. Temperature control was achieved with a Lauda K-2/R circulating constant temperature bath attached to thermostatable UV cell holders. High-pressure liquid chromatographic (HPLC) analyses were carried out on a Beckman 324 gradient liquid chromatograph using an Altex Ultrasphere-ODS preparative (10 mm × 25 cm) column.

The hydrochloride salts of hydrazines **17**[24] and **20**[25] were prepared according to published procedures. Dimethyl acetylenedicarboxylate (DMAD) and triethylamine were purified by vacuum transfer from calcium hydride. Triphenylphosphine was purified by recrystallization from petroleum ether, trimethylphosphine (Strem) was vacuum transferred but otherwise used as received, trimethylphosphite was degassed by three freeze–pump–thaw cycles, and tricyclohexylphosphine (Orgmet) was used as received. Ferrocene was purified by sublimation. Dioxane was purified by distillation from sodium benzophenone ketyl. *tert*-Butyl hypochlorite was purchased from Chemical Dynamics Corp. and used without further purification or degassing.

Syntheses of the dinuclear compounds **1**, **5**, **9**, and **10** were accomplished as described in the preceding paper.[8] The dimetallacycles used were recrystallized from methylene chloride/pentane.

(η^5-Methylcyclopentadienyl)carbonyl(dimethylphenylphosphine)cobalt. A mixture of 0.5 g of $MeCpCo(CO)_2$[8] (2.2 mmol) and 0.4 g of $PPhMe_2$ (2.9 mmol) in 10 mL of benzene was degassed and heated at 40 °C for 3 days in a glass bomb sealed with a Teflon-brand vacuum stopcock. After solvent removal, the resultant viscous red oil was applied in hexane to a silica chromatography column. After washing with hexane, a single red band was eluted with hexane/benzene. Solvent removal in vacuo gave 520 mg (78% yield) of a low-melting air-sensitive red solid: mp ~25 °C; MS (EI), *m/e* 304 (M^+), 276 ($M^+ - CO$); IR (hexane) 1935 (s) cm^{-1}; ^{1}H NMR (C_6D_6) δ 7.57 (m, 2 H), 7.07 (m, 3 H), 4.76 (t, J = 1.9 Hz, 2 H), 4.26 (q, J = 2.2 Hz, 2 H), 1.85 (d, J = 1.0 Hz, 3 H), 1.31 (d, J = 8.8 Hz, 6 H). Anal. Calcd for $C_{15}H_{18}OPCo$: C, 59.22; H, 5.96; P, 10.18. Found: C, 59.00; H, 5.96; P, 10.21.

α,α'-Dibromo-*o*-xylene-d_8. Starting with 5 g of *o*-xylene-d_{10} (Aldrich), the literature procedure[26] for the protio material was followed to give 3.8 g of product (33% yield) after recrystallization: mp 91–93.5 °C (lit.[26] 93–4 °C).

(μ-*o*-Xylylene)(η^5-cyclopentadienyl)(η^5-methylcyclopentadienyl)bis(μ-carbonyl)dicobalt (14). A mixture of three radical anions (Na[CpCo(CO)]$_2$, Na[MeCpCpCo$_2$(CO)$_2$], and Na[MeCpCo(CO)]$_2$) was prepared by sodium amalgam reduction[27] of a mixture containing 44% $CpCo(CO)_2$ and 56% $MeCpCo(CO)_2$. Dropwise treatment of a suspension of 1.47 g of this material (3 mmol) in 25 mL of THF with a solution of 0.83 g of α,α'-dibromo-*o*-xylene in 10 mL of THF resulted in a color change from dark green to blue-green to olive-green. Immediately upon completion of the addition, 25 mL of hexane was added; the mixture was filtered through a frit and then filtered through an alumina column. A small red forerun was discarded, after which the column was washed with benzene to give a green fraction. After solvent removal in vacuo, the residue was chromatographed on alumina. Elution with hexane yielded a red dicarbonyl band, and elution with benzene yielded a green band that was collected in three fractions. Removal of the frozen solvent by sublimation gave 310 mg (24% yield) of the mixed dimetallacycles as a dark green powder.

The dimetallacycles were analyzed by HPLC, eluting with acetonitrile. Authentic bis(cyclopentadienyl) dimetallacycle **1** was eluted in 3.7 min under the flow conditions used, while bis(methylcyclopentadienyl) dimetallacycle **5** eluted in 4.2 min. Analysis of the dimetallacycle mixture revealed in addition to these two bands a major new band of intermediate polarity at 3.9 min. Elution with 90% MeCN/10% H_2O gave base-line resolution, the three peaks eluting in 4.7, 5.3, and 6.1 min. Analysis of the three fractions taken from the alumina chromatography revealed that some fractionation had taken place: the first fraction contained the most **1**, the second the most **14** (about 50% of the total), and the third the most **5**.

The ^{1}H NMR was also consistent with the formation of mixed dimetallacycle **14**; integration of the spectrum of the second chromatography fraction indicated that the mixture contained 20% **1**, 29% **5**, and 51% **14**: ^{1}H NMR (C_6D_6) δ 7.04 (s, aromatic CH, **1**, **5**, **14**), 4.59 (s, Cp, **14**), 4.57 (s, Cp, **1**), 4.44 (t, J = 2.1 Hz, Me*Cp*, **5**), 4.42 (t, J = 2.1 Hz, Me*Cp*, **14**), 4.32 (t, J = 2.0 Hz, Me*Cp*, **5**), 4.30 (t, J = 2.0 Hz, Me*Cp*, **14**), 1.77 (s, *Me*Cp, **5**), 1.74 (s, *Me*Cp, **14**), 1.72 (s, CH_2, **14**), 1.70 (s, CH_2, **1**), 1.60 (s, CH_2, **5**), 1.59 (s, CH_2, **14**).

$Cp_2Co_2(CO)_2$(DMAD) (16). A solution of 15 mg of DMAD (0.11 mmol) in 2 mL of ether was added to a solution of 32 mg of **9** (0.11 mmol) in 10 mL of ether. After stirring for 1 min, the solvent was removed from the deep red solution in vacuo. The resulting brown powder was taken up in 5 mL of ether, concentrated to about 0.5 mL, and cooled to −78 °C to yield 10 mg of 16 (21% yield) as small, air-stable, black crystals: IR (ether) 1996 (s), 1963 (w, br), 1790 (m, br), 1725 (m, br) cm^{-1}; IR (KBr) 1989 (s), 1945 (w), 1797 (ms, br), 1787 (ms, shoulder), 1716 (ms), 1709 (ms) cm^{-1}; ^{1}H NMR (C_6D_6, 22 °C) δ 4.91 (br s, 5 H), 4.28 (br s, 5 H), 3.79 (br s, 3 H), 3.32 (br s, 3 H).

Allowing a toluene solution of 16 to stand overnight at room temperature gave, after addition of hexane and cooling to −40 °C, a 40% yield of small black-green crystals: IR (ether) 1990 (s), 1793 (w, br), 1726 (m), 1715 (m), 1555 (w) cm^{-1}; IR (KBr) 1977 (vs), 1784 (w), 1709 (s), 1545 (m) cm^{-1}; ^{1}H NMR (C_6D_6) 12% of the sample is 16, the rest is δ 4.69 (s, 10 H), 3.59 (s, 6 H). The IR spectrum of DMAD itself (in ether) contains a very strong band at 1733 cm^{-1} as the only prominent feature.

$MeCp_2Co_2(CO)_2$(DMAD). A mixture of 54 mg of **10** (0.16 mmol) and 23 mg of DMAD (0.16 mmol) were allowed to react in 10 mL of ether for 1 min. After solvent removal in vacuo, the residue was taken up in 6 mL of a 1:1 mixture of ether and *n*-pentane. Slow cooling to −40 °C gave 57 mg (76% yield) of large long black needles. This material turned out to consist of thin-walled, hollow tubes, and repeated attempts to grow solid needles at higher temperatures in more dilute solutions still gave hollow tubes: mp 77–80 °C; MS (CI), *m/e* 475 ($M + H^+$), 447 ($M - CO + H^+$), 419 ($M - 2CO + H^+$); IR (ether) 1996 (s), 1781 (m), 1722 (m) cm^{-1}; ^{1}H NMR (toluene-d_8) δ 5.02 (t, J = 1.6 Hz, 2 H), 4.69 (q, J = 2.3 Hz, 1 H), 4.45 (br s, 1 H) (all due to one Me*Cp*), 4.24 (br s, 2 H), 4.16 (br s, 2 H) (both due to the other Me*Cp*), 3.77 (br s, 3 H), 3.31 (br s, 3 H) (MeO), 1.74 (br s, 3 H), 1.57 (br s, 3 H) (*Me*Cp). Anal. Calcd for $C_{20}H_{20}O_6Co_2$: C, 50.65; H, 4.25. Found: C, 50.91; H, 4.46.

Warming this compound in the NMR probe to 50 °C led to severe broadening of all the peaks, including formation of one broad singlet for the high-field Me*Cp* at δ 4.25. At 60 °C the *Me*Cp signals had merged into a broad singlet and all of the Me*Cp* signals were broadening into each other. Cooling back to room temperature showed that about 15% of the starting material had decomposed. The major prominent new peaks, especially on continued heating, were a new MeO singlet at δ 3.59 and a new *Me*Cp singlet at 1.74.

***N*-Aminodihydroisoindole (17).** The free amine was prepared by stirring 0.52 g of the hydrochloride salt[25] (3.1 mmol) in a solution of 0.53 g of KOH (9.5 mmol) in 25 mL of nitrogen-purged water. The aqueous mixture was extracted 5 times with nitrogen-purged ether and 2 more times with nitrogen-purged methylene chloride. After drying briefly over molecular sieves, the solvent was removed in vacuo to give 216 mg (53% yield) of white flakes. The slightly air-sensitive free amine sublimed readily at 30 °C (0.002 mm), to give the analytically pure material: mp 64–65.5 °C; MS (EI), *m/e* 134 (M^+); ^{1}H NMR (C_6D_6) δ 6.96 (AA′BB′, 4 H), 3.80 (s, 4 H), 2.75 (br s, 2 H). Anal. Calcd for $C_8H_{10}N_2$: C, 71.61; H, 7.52; N, 20.88. Found: C, 71.67; H, 7.53; N, 20.66.

1,2,3,4-Tetrahydrophthalazine (20). The hydrochloride salt of **20**, described in the literature[25] as the monohydrochloride (mp 236–238 °C) was obtained as the bis(hydrochloride), on the basis of chlorine analysis (mp 233–238 °C). The free hydrazine was obtained by stirring 252 mg of the salt (1.2 mmol) in 10 mL of 1 N KOH solution, in the presence of nitrogen-purged ether. After extraction with 4 × 25 mL of ether, the combined organic phases were concentrated to give a yellow oil. After dissolving in the minimum amount of ether, cooling to −40 °C gave 68 mg (42% yield) of air-sensitive white plates. Sublimation as described for **17** gave analytically pure material: mp 56–60 °C; MS (EI), *m/e* 134 (M^+); ^{1}H NMR (C_6D_6) δ 6.87 (AA′BB′, 4 H), 3.66 (s, 4 H); 2.84 (br s, 2 H). Anal. Calcd for $C_8H_{10}N_2$: C, 71.61; H, 7.52; N, 20.88. Found: C, 71.33; H, 7.47; N, 20.59.

Reactions of 9 with 10, $MeCpCo(CO)PPhMe_2$, and $PPhMe_2$. These reactions were call carried out at room temperature by mixing the reactants with 3–5 mg of 9 in 0.6–0.8 mL of C_6D_6 in the drybox followed by transfer of the mixtures to NMR tubes that were then simply capped. For $MeCpCo(CO)PPhMe_2$, no reaction of **9** with 15 equiv of the carbonylphosphine was observed after 2 h. The reactions of **9** (and/or **10**)

(24) Carpino, L. A. *J. Am. Chem. Soc.* **1957**, *79*, 4427–4431.
(25) Carpino, L. A. *J. Am. Chem. Soc.* **1963**, *85*, 2144–2149.
(26) Stephenson, E. F. M. "Organic Syntheses"; Wiley: New York, 1963; Collect. Vol. 4, pp 984–986.
(27) Schore, N. E.; Ilenda, C. S.; Bergman, R. G. *J. Am. Chem. Soc.* **1977**, *99*, 1781–1787.
(28) Butler, D. N.; Snow, R. A. *Can. J. Chem.* **1975** (1), *53*, 256–262.

with $PPhMe_2$ were carried out by addition of roughly 3 equiv of the phosphine (6–12 μL) to the neutral dimer(s). The NMR results are compiled in Table II.

Crossover Reaction of 1-d_8, 5-d_8, and $PPhMe_2$. The two metallacycles (3 mg each) were dissolved in 0.6 mL of C_6D_6; 5 μL of $PPhMe_2$ was then added. After 15 min of reaction, the mixture consisted of 5% **1**, 19% **5**, 41% **2**, and 36% 6. After 45 min, no **1** and 3% of **5** remained. A residual shoulder peak at δ 2.07 (possibly due to **8**) was 0.9 ± 0.1 mol % of 6, while a residual peak at δ 4.96 (possibly due to **7**) was 2.8 ± 1.4 mol % of **2**. Hence the maximum amount of **7** and **8** relative to **2** and 6 was 1.9 ± 0.7 mol %.

Reaction of 1 and DMAD. A mixture of 4.5 mg of 1 (0.01 mmol) and 10 μL of DMAD (0.08 mmol) in about 0.7 mL of C_6D_6 slowly turned color from olive-green to dark red, over the course of 30 min. ^1H NMR showed that the starting material had disappeared. Peaks were observed due to excess DMAD (δ 3.02, s), **16** (see above), and Diels–Alder adduct **15** (δ 6.87 (AA'BB', 4 H), 3.45 (s, 10 H); lit.[28] (CCl_4) δ 7.14 (s, 4 H), 3.77 (s, 6 H), 3.64 (s, 4 H)). The integrated ratio of **15**/**16** was 1.2:1. Several minor peaks were also observed, at δ 4.69, 4.40, 4.34, 3.40, and 3.35, apparently due to secondary thermal decomposition of **16** and to the DMAD trimer hexakis(methoxycarbonyl)benzene, observed as the singlet at δ 3.40. These minor peaks increased in intensity when the solution was warmed to 40 °C, and that assumed to be due to the DMAD trimer increased as long as excess DMAD was present.

In THF-d_8, the Cp peaks of **16** appeared at δ 5.04 and 4.81 as broad (especially the higher field peak) singlets, while the methoxycarbonyl signals were not observed and may be coincident with that due to free DMAD at 3.79. Diels–Alder adduct **15** was observed as three singlets at δ 7.15 (4 H), 3.73 (6 H), and 3.67 (4 H); again the integrated ratio of **15**/16 was 1.2:1. The signals due to **15** remained unchanged after 4 h at room temperature, and again several small singlets grew in, at δ 5.13 (possibly $CpCo(CO)_2$), 5.06, 4.92, 4.87, 4.46, and 3.82 (possibly the DMAD trimer).

Reaction of 9 with 17. Control experiments showed that **17** could be oxidized by brown mercuric oxide[20] prepared as described in the literature[29] but not by commercially available material. Thus, addition of excess brown HgO to **17** in C_6D_6 at room temperature gave rise to gas evolution that subsided after about 20 min. After drying ($MgSO_4$) and filtering, a high yield of spiro dimer **4b** was obtained.

In a similar manner, brown HgO was added to a solution of 4 mg of **9** (0.013 mmol) and 2 mg of **17** (0.015 mmol) in 0.3 mL of C_6D_6. After 20 min, the mixture had turned brown-orange and the bubbling had subsided. Workup as above gave rise to the ^1H NMR spectrum described in the text.

Reaction of 9 with 20. In a control experiment, 1.9 mg of **20** (0.014 mmol) and 2.2 μL of NEt_3 (0.016 mmol) in 6 mL of THF were cooled to −75 °C after which 2.2 μL of *tert*-butyl hypochlorite (0.018 mmol) was added via syringe. The stirred reaction mixture was then allowed to warm to room temperture. After solvent removal, extraction of the resultant white solid with C_6D_6, and addition of methylene chloride as an internal standard, NMR analysis indicated that spiro dimer **4b** had been obtained in about 80% yield.

In a similar manner, 4.9 mg of **20** (0.037 mmol) and 7.0 μL of NEt_3 (0.050 mmol) in 12 mL of THF were cooled in a Schlenk flask to −90 °C; 6 μL of *tert*-butyl hypochlorite (0.05 mmol) was then added via syringe in one portion. After stirring at −90 °C for 5 min, a cold solution of 11.5 mg of **9** (0.038 mmol) in 4 mL of THF was added via syringe. The first few drops were decolorized instantly, presumably due to reaction of **9** with excess hypochlorite. After stirring for about 1 min at −90 °C, the cold bath was removed and the mixture allowed to warm rapidly to room temperature. During this warmup, the color changed from the blue-green of **9** to the olive-green of **1**. Following solvent removal in vacuo, the resultant olive-green residue was taken up in C_6D_6 and 5.2 mg of ferrocene added as an internal standard. The only peaks observed in the NMR were at δ 7.03 (s, 4 H, **1**), 4.61 (s, 3% of Cp, $[CpCo(CO)]_3$), 4.57 (s, 10 H, 81% of Cp, 1), 4.40 (s, 16% of Cp, **9** and/or $CpCo(CO)_2$), 4.00 (s, Cp_2Fe), and 1.69 (s, 4 H, **1**). This mixture was poured onto a 7-cm column of alumina II in a disposable pipette; after elution with hexane to remove ferrocene, $CpCo(CO)_2$, and any **9** that might have remained (a small green fraction was discarded), an intense green fraction was eluted with benzene. After removal of the solvent by sublimation, 5 mg (34% yield) of spectroscopically pure **1** was obtained as a green powder.

Reactions of **9** and **20** on an NMR scale were carried out, at roughly double the above concentrations, by addition of *tert*-butyl hypochlorite (0.8 μL) to a solution of 1 mg of **20** and 1 μL of NEt_3 in 0.75 g of THF-d_8 in a septum-capped NMR tube at −90 °C, followed by addition of a solution of 2 mg of **9** and 1 mg of ferrocene in 0.25 g of THF-d_8. Rapid warming to room temperature gave rise to an NMR spectrum indicating a 38 ± 5% recovery of organometallic products, 31% of which was **1**. The remainder was apparently $CpCo(CO)_2$ (58%) and two unidentified products.

Two similar experiments, in which the reaction was monitored by NMR starting at −65 °C, were carried out. These gave reproducible results: at −65 °C, **19** was present (δ 7.29 (s, 4 H), 4.91 (s, 4 H), as confirmed by a control experiment; lit.[22] (acetone-d_6) δ 7.41, 5.04), and peaks at δ 5.22 (29% of Cp, possibly $CpCo(CO)_2$), 5.01 (7%), 4.76 (57%, **9**), and 4.72 (7%) were observed. Warming to −50 °C resulted in disappearance of **19** with formation of **1** (δ 5.14) and more of the unidentified materials. The final room-temperature spectrum (which did not change on recooling) contained Cp peaks at δ 5.14 (54%, possibly $CpCo(CO)_2$), 5.09 (13%, **1**), 4.98 (3%), 4.88 (11%), and 4.71 (19%, **9**); the recovery of organometallic products was 38 ± 7%. In addition to the complex changes in the cyclopentadienyl region of the spectrum, a large new aromatic AA'BB' multiplet grew in centered at δ 6.46; it was clearly visible at −50 °C and persisted at room temperature. It was roughly 6 times as large as the AA'BB' multiplet due to 1 centered at δ 6.76, and was also observed (in roughly a 1.5:1 ratio) in the NMR experiment described above in which the reaction mixture was rapidly warmed to room temperature. The unusual chemical shift (compare also **19**, singlet at 7.29, and **20**, AA'BB' centered at δ 7.02) and size indicate that this signal may be due to a new organometallic product that has a Cp resonance in the same place as $CpCo(CO)_2$; in addition the color of the final solution is light green rather than the orange of $CpCo(CO)_2$.

NMR Kinetics. Samples for kinetic analysis by ^1H NMR were prepared in one of two ways. The first method was used for the reaction of phosphines (PPh_3, PCy_3, and PMe_3) with metallacycle 1, while the second was used for the reactions of $P(OMe)_3$, DMAD, and neutral dimer **10** with 1, as well as for the neutral dimer scrambling reaction of **9** and **10**.

In the first method, an NMR tube fused to a 14/20 ground-glass joint was charged with weighed amounts of **1**, ferrocene, and PPh_3 or PCy_3 (the latter always in the drybox). The tube was then fitted with a Teflon-brand vacuum stopcock, attached to a high-vacuum manifold, and evacuated. THF-d_8 was then added by vacuum transfer, with care being taken to wash any reactants away from the area that would later be flame sealed. In the case of PMe_3, this reactant was then added by vacuum transfer from a known-volume bulb. After once more applying a vacuum to the frozen sample, the tube was sealed with a torch. Samples were kept frozen in liquid nitrogen until immediately prior to use, when they were thawed rapidly in the air.

In the second method, the samples were prepared in the drybox. For the $P(OMe)_3$ and DMAD reactions, a THF solution of 1 and ferrocene was filtered into an NMR tube that had been placed in a bath of toluene that had been precooled to −40 °C. The reactant was then added via syringe (in the case of the 1 M DMAD reaction, a weighed sample in THF-d_8 was used) to the cold solution, after which the tube was rapidly capped with a polyethylene NMR cap, removed from the drybox, and placed in a dry ice/acetone cold bath. The sample was further sealed by then wrapping the cap with parafilm. The unfrozen samples were warmed in the air immediately prior to use. For the reaction of **10** with **1**, this procedure was altered only in that a cold solution of **10** was added to solid **1** in the NMR tube, while in the case of the reaction of **9** and **10**, it was altered only in that cold solutions of **9** and **10** were added sequentially to the NMR tube.

All reactions were carried out under pseudo-first-order conditions, using (except as noted below) a minimum of 5 equiv of the excess reactant. In the case of the phosphine and DMAD reactions, this corresponded to a 10-fold molar excess, since the overall reaction stoichiometry requires 2 equiv of PR_3 or DMAD per mole of **1**. The reactions between **1** and **10** also used a 10-fold molar excess—that is, 10 equiv of **10** were used instead of 5. Reactant concentrations were determined by measuring the solution height in the NMR tubes immediately after removing the samples from the NMR probe; these heights were converted to the required volumes by using the formula $V = \pi(0.21)^2h$, where h is the solution height and the NMR tube radius is 0.21 cm. The values so obtained were indistinguishable from those determined by comparison of the heights to those of known volumes. In general, from 0.55 to 1 mL of solution was used, concentrations of 1 ranged from 0.001 to 0.048 M, and ligand concentrations ranged from 0.009 to 1.5 M.

The reaction temperature—that is, the temperature in the NMR probe—was controlled by a nitrogen flow system and was measured immediately prior to each kinetic run by means of a methanol standard sample and the calibration of van Geet.[30] This sample was found to equilibrate within 1 min when warmed from −196 or −78 °C in the air

(29) Carpino, L. A.; Santilli, A. A.; Murray, R. W. *J. Am. Chem. Soc.* **1960**, *82*, 2728–2731.

(30) van Geet, A. L. *Anal. Chem.* **1970**, *42*, 679–680.

and placed in the NMR probe, as described above for the kinetic samples.

All spectra were acquired and stored under computer control, in such a manner as to obtain 10–25 spectra over the course of 3–4 reaction half-lives. For the reaction between **9** and **10**, disappearance of the methyl signal of **10** at δ 1.673 was monitored; the product methyl signal of **11** grew in at δ 1.625. The higher field signal due to the residual hydrogen in the THF-d_8 solvent was used as an internal integration standard (see below). For the reactions of **1** with phosphines, DMAD, and **10**, the disappearance of the Cp singlet of **1** relative to ferrocene as the internal standard (except as noted below) was monitored. For the high-concentration runs using DMAD, the intense DMAD signal precluded accurate monitoring in the Cp region, so in these cases the rate of disappearance of the methylene singlet of **1** relative to the residual THF protons was monitored. The rates could be measured in both ways for the low-concentration DMAD runs, and they were the same, confirming the accuracy of the THF internal standard. Dioxane was used as the internal standard in the low-temperature reaction between **1** and **10**, while the THF residual signal was again used in the room-temperature reactions. Least-squares fitting of the data to first-order plots of the disappearance of **1** gave straight lines generally having standard deviations of ±1–4%.

UV–Visible Kinetics. Two standard stock solutions of **1**, 1.1×10^{-4} and 2.5×10^{-3} M, in THF were prepared and stored, without detectable decomposition, at −40 °C. THF solutions of DMAD and $P(OMe)_3$ were prepared by adding THF to weighed amounts of each compound in volumetric flasks at room temperature. The densities of these solutions were then determined, after which they were cooled to −40 °C.

Immediately prior to use, cold solutions of **1** and DMAD or $P(OMe)_3$ were weighed (in the drybox) into a 1-cm path-length quartz UV cuvette that was fused to a Teflon-brand vacuum stopcock. Room-temperature concentrations were calculated from the known weights and densities. After closing the stopcock, the cuvette was rapidly removed from the box and stored in a −15 °C cold bath. No detectable decomposition occurred at this temperature. The reactions were initially examined with the Hewlett-Packard instrument and appeared well-behaved; the DMAD reaction exhibited isosbestic points at about 310, 450, and 600 nm. For kinetic runs the Carey was used, by monitoring at a single wavelength as described in the text. Temperatures were measured with a calibrated thermometer inserted into a similar quartz UV cell containing THF; it was found that 1 min of shaking the sample cell in a water bath held at the same temperature as the cell holders was necessary for equilibration.

Generally about 30 absorbance readings over 4–5 half-lives were used to determine the reaction rate; for most reactions the rates were sufficiently rapid that end-point readings could be made after 10 half-lives without removing the cuvette from the machine. First-order reaction rates were obtained by plots of ln $(A_t - A_\infty)$ vs. time. The end point used (except as noted below) was that which gave the minimum standard deviation from the least-squares fit to a straight line, but these calculated end points did not differ appreciably from the observed values. The observed standard deviations of the first-order reaction rates were ±0.1–1.0%. For the 0.5 M DMAD, 0.001 M **1** sample, as well as the other 0.001 M **1** samples, which were not first order, the observed end points were used, since varying these end points did not result in minima in the standard deviations; even so the deviations were only ±0.4–1.7%.

Acknowledgment. Financial support for this work was provided by National Science Foundation Grant CHE79-26291. W.H.H. acknowledges an NIH National Research Service Award (F32-GM-07539) from the National Institute of General Medical Sciences. R.G.B. acknowledges a Research Professorship (1982–1983) from the Miller Institute for Basic Research at U. C. Berkeley.

Registry No. 1, 79931-94-5; **4a**, 1460-59-9; **4b**, 4968-91-6; **5**, 86364-95-6; **9**, 58496-39-2; **10**, 86364-96-7; **11**, 86455-89-2; **12**, 79931-95-6; **13**, 12078-25-0; **14**, 86437-13-0; **15**, 56306-55-9; **16**, 86437-14-1; **17**, 21507-95-9; **17**·HCl, 86437-17-4; **20**, 13152-89-1; **20**·HCl, 86437-12-9; $MeCpCo(CO)_2$, 75297-02-8; $Na[CpCo(CO)]_2$, 62602-00-0; $Na[MeCpCo_2(CO)_2]$, 86437-15-2; $Na[MeCpCo(CO)]_2$, 86364-94-5; $MeCp_2Co_2(CO)_2$(DMAD), 86437-16-3; Co, 7440-48-4; $PPhMe_2$, 672-66-2; PPh_3, 603-35-0; PCy_3, 2622-14-2; PMe_3, 594-09-2; $P(OMe)_3$, 121-45-9; DMAD, 762-42-5; (η^5-methylcyclopentadienyl)carbonyl(dimethylphenylphosphine)cobalt, 86364-98-9; α,α'-dibromo-*o*-xylene, 91-13-4; α,α'-dibromo-*o*-xylene-d_8, 86437-11-8; *o*-xylene-d_{10}, 56004-61-6.

Accessibility of Triplet Indenylidene in Solution

Robert A. Moss* and Claire M. Young[1]

Contribution from the Wright and Rieman Laboratories, Department of Chemistry, Rutgers, The State University of New Jersey, New Brunswick, New Jersey 08903. *Received January 24, 1983*

Abstract: Photolysis of diazoindene generated indenylidene (**2**), which reacted with isobutene, *cis*-butene, and *trans*-butene, forming adducts **5a–c** and insertion products **6a–c**. NMR-based configurational assignments to cyclopropanes **5b-*syn***, **5b-*anti***, and **5c** permitted detailed analysis of the stereochemistry of addition of **2** to *cis*- and *trans*-butene. The stereochemistry was studied as a function of dilution of the alkenes with *c*-C_4F_8 or 2,3-dimethylbutadiene. These experiments clarified the product-forming roles of singlet and triplet **2**. In the presence of 97 mol % *c*-C_4F_8, ~47% of the cyclopropanes derived from **2** and *cis*-butene came from triplet **2**. Triplet reactions were almost entirely eliminated in the presence of 25 mol % of 2,3-dimethylbutadiene. The reactions of the butene olefins with **2** were compared to similar reactions with cyclopentadienylidene (**1**) and fluorenylidene (**3**).

The triad of carbenes cyclopentadienylidene (**1**), indenylidene (**2**), and fluorenylidene (**3**) invites investigation because connec-

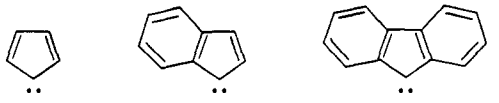

1 2 3

tions between structure, spin state, and reactivity might be particularly clear. All these carbenes are ground-state triplets, as shown by electron spin resonance studies.[2] Cyclopentadienylidene, generated as the singlet by photolysis of diazocyclopentadiene, is a highly reactive, electrophilic species that displays low selectivity in its reactions with alkanes, alkenes, and sulfides.[3] Reactions

(1) Special graduate school fellow, Rutgers University.

(2) Trozzolo, A. M.; Murray, R. W.; Wasserman, E. *J. Am. Chem. Soc.* **1962**, *84*, 4990. Wasserman, E.; Barash, L.; Trozzolo, A. M.; Murray, R. W.; Yager, W. A. *Ibid.* **1964**, *86*, 2304.

(3) (a) Moss, R. A.; *J. Org. Chem.* **1966**, *31*, 3296. (b) Ando, W.; Saiki, Y.; Migita, T. *Tetrahedron* **1973**, *29*, 3511. (c) Dürr, H.; Werndorff, F. *Angew. Chem., Int. Ed. Engl.* **1974**, *13*, 483. (d) Migita, T.; Kurino, K.; Ando, W. *J. Chem. Soc., Perkin Trans. 2* **1977**, 1094. (e) Baird, M. S.; Dunkin, I. R.; Hacker, N.; Poliakoff, M.; Turner, J. J. *J. Am. Chem. Soc.* **1981**, *103*, 5190.

0002-7863/83/1505-5859$01.50/0